AD_____

Award Number:

W81XWH-09-1-0673

TITLE:

IL-6 Receptor Isoforms and Ovarian Cancer Progression

PRINCIPAL INVESTIGATOR:
Angela F. Drew, Ph.D.

CONTRACTING ORGANIZATION:
University of Cincinnati

Cincinnati OH 45221-0001

REPORT DATE:
October 2010

TYPE OF REPORT:
Annual

PREPARED FOR: U.S. Army Medical Research and Materiel Command
Fort Detrick, Maryland 21702-5012

DISTRIBUTION STATEMENT:

X Approved for public release; distribution unlimited

□

REPORT DOCUMENTATION PAGE

Form Approved
OMB No. 0704-0188

1. REPORT DATE *(DD-MM-YYYY)*	2. REPORT TYPE	3. DATES COVERED *(From - To)*
01-10-2010	Annual	15 SEP 2009 - 14 SEP 2010

4. TITLE AND SUBTITLE
IL-6 Receptor Isoforms and Ovarian Cancer Progression

5a. CONTRACT NUMBER

5b. GRANT NUMBER
W81XWH-09-1-0673

5c. PROGRAM ELEMENT NUMBER

6. AUTHOR(S)
Drew, Angela F.

5d. PROJECT NUMBER

5e. TASK NUMBER

5f. WORK UNIT NUMBER

7. PERFORMING ORGANIZATION NAME(S) AND ADDRESS(ES)
University of Cincinnati

Cincinnati OH 45221-0001

8. PERFORMING ORGANIZATION REPORT NUMBER

9. SPONSORING / MONITORING AGENCY NAME(S) AND ADDRESS(ES)
U.S. Army Medical Research and Materiel Command
Fort Detrick, Maryland 21702-5012

10. SPONSOR/MONITOR'S ACRONYM(S)

11. SPONSOR/MONITOR'S REPORT NUMBER(S)

12. DISTRIBUTION / AVAILABILITY STATEMENT
Approved for public release; distribution unlimited

13. SUPPLEMENTARY NOTES

14. ABSTRACT

During the research period, we have successfully achieved our goals of demonstrating IL6R in the ovarian tumor microenvironment and identifying the differentially-spliced isoform as being prominent. In addition, we have demonstrated an important relationship between IL6R expression and the earliest steps in metastasis of ovarian cancer. Both tumor cells and host myeloid cells contribute to IL6R expression within a tumor, thus providing multiple targets for intervening in ovarian cancer metastasis. Our continuing studies will identify the mechanism by which IL6R influences metastasis and opportunities for preventing or reducing this outcome.

15. SUBJECT TERMS
IL-6 Receptor, inflammation, ovarian cancer, metastasis

16. SECURITY CLASSIFICATION OF:			17. LIMITATION OF ABSTRACT	18. NUMBER OF PAGES	19a. NAME OF RESPONSIBLE PERSON
a. REPORT	b. ABSTRACT	c. THIS PAGE			USAMRMC
U	U	U	UU	26	19b. TELEPHONE NUMBER *(include area code)*

Table of Contents

Page

INTRODUCTION:

Interleukin-6 (IL6) is an inflammatory cytokine that plays numerous roles in the tumor microenvironment influencing tumor cell proliferation, survival, migration and effects on stromal cells. Some of the effects of IL6 signaling, mediated through a specific receptor (IL6R), can have a positive or negative effect on tumor progression. In this study, we attempt to elucidate the pleiotropic effects of IL6 signaling in several models of ovarian cancer, with the ultimate aim of specifically targeting the protumor effects and hence reducing the mortality associated with this disease. To do this, we investigate the effects of both tumor cell and host stromal production and response to IL6R. We investigate the effects of the various IL6R isoforms in altering the progression of ovarian cancer. The goal is to specifically target the effects of IL6 signaling that facilitate ovarian tumor metastasis.

BODY:

Statement of Work

Task 1. Identification of IL-6R isoforms in patient samples (Months 1 – 12).

(i) RNA isolation and real-time PCR analysis of patient samples

It is well known that IL6 expression in patients is associated with increasing stage of ovarian cancer. However, it was not clear whether the expression of IL6R, a necessary component of IL6 signaling, was also increased. We isolated RNA from non-tumor nearing ovaries and from patient ovarian cancer samples, and performed real-time PCR analysis on these samples. We found a dramatic upregulation of IL6R in advanced ovarian cancer samples compared with benign ovaries (Figure 1, Rath et al., 2010 (*1*), Appendix 1). In addition, we confirmed increased IL6 expression in advanced cancers. These findings indicate the relevance of IL6 signaling in the ovarian tumor microenvironment.

In our further analyses, we used Q-PCR primers specific for the full length and differentially-spliced isoforms of IL6R to identify which isoform was more prevalent in ovarian tumors. Somewhat surprisingly, we found that both malignant tumor samples from patients and ovarian carcinoma cell lines expressed greater amounts of the differentially spliced isoform than any other tissue studied to date, including liver, immune cells or benign ovaries (Figure 2, (*1*)). Liver and immune cells are known to be the major sources of IL6R in the obdy. The implications of this finding are that tumors contribute additional IL6R to their microenvironment in the form of the less common differentially-spliced variant.

(ii) and (iii) Protein analyses including immunohistochemistry and in situ hybridization of IL6R isoforms in patient samples.

We have performed sectioning and immunohistochemistry on patient ovarian cancer samples to localize IL6R expression within the tumor. Towards this end, we have demonstrated that IL6R was only expressed in the surface epithelium of benign ovaries and absent from the stroma, the

major constituent of non-tumor-bearing ovaries. In ovaries bearing epithelial malignancies, we showed that IL6R once again localized to the epithelium and not the tumor stroma (Figure 1C and D, Rath etal., 2010). Given that the epithelial tumor cells constitute most of the ovarian tissue in advanced stage tumors, IL6R expression was therefore greatly increased in malignant ovarian samples, consistent with the RNA data obtained earlier. The successful localization of IL6R expression obviated the need for in situ hybridization analysis.

We had proposed the usage of an antibody (2F3) reported to specifically identify the differentially-spliced form of IL6R (*2*). We obtained this antibody from the reporting investigator and performed rigorous testing of the specificity of this antibody. Unfortunately, we could not demonstrate specificity of this antibody for the differentially-spliced isoform of IL6R. To the best of our knowledge, no other antibody has reported to fulfill this purpose so this confirmatory study has not been continued at this point. However, combining the abovementioned results, we have obtained sufficient data to demonstrate that IL6R expression in tumors localizes to the epithelial ovarian tumor cells, and that it is the differentially-spliced isoform that is greatly upregulated.

Task 2. In vivo experiments to determine functions of IL-6R isoforms and tumor:stroma relationship (Months 4-24)

(i) Increase mouse breeding and genotyping to ensure sufficient numbers of mice for experiments.

Mouse breeding and genotyping have been sufficiently increased to provide adequate numbers of mice in the following colonies: wild-type, $IL6^{-/-}$, $IL6R^{-/-}$, $IL6R^{fl/fl}$, $LysMCre^{+}/IL\text{-}6R^{fl/fl}$, $AlbCre^{+}/IL\text{-}6R^{fl/fl}$. In addition, we have characterized the general phenotype of all of these mice (McFarland-Mancini et al., 2010 (*3*); Appendix 2).

(ii) Implant KD and control tumor cells into the ovaries of groups of 10 SCID or C57Bl6 mice followed by monitoring and necropsy.

Towards this end we have generated ovarian carcinoma cell lines overexpressing IL6R, with knockdown of IL6R, and control vector-expressing lines for each. These cells have been implanted into the ovaries of mice. We have made the novel finding that tumor cell expression of IL6R greatly enhances the earliest metastases of ovarian cancer to the omentum. It has previously been demonstrated that the omentum is among the earliest sites in which ovarian metastases are observed and is a preferred site for metastases(*4*). We have previously shown similar metastatic dissemination patterns in mouse models (*5*). We are now undertaking detailed studies to identify which IL6 downstream signaling pathways are required for this effect and which of the downstream candidate molecules we have identified are involved. This study will provide a target for blocking the protumor effects of IL6R.

(iii) Implant tumor cells into groups of 10 IL-6R-/-, LysMCre $IL\text{-}6R^{-/-}$, AlbCre $IL\text{-}6R^{-/-}$ and wild type mice followed by monitoring and necropsy.

This experiment has been performed and indicates that not only is host IL6R influential in tumor progression, but that myeloid sources (macrophages) are more directly involved than hepatic IL6R. Current experiments are underway to determine whether myeloid cells in the omentum, peritoneum or periphery are more relevant. These experiments provide a rationale for targeting host IL6R isoforms. Further, our xenograft studies have shown that host IL6R is another means by which IL6R levels are increased in the ovarian tumor microenvironment.

(iv) Reconstitution (soluble IL-6R and gp130) in IL-6-/- and wild type mice; tumor implantation, monitoring and necropsy.

Mice have been generated for this experiment and soluble recombinant proteins have been purchased. Experiments will commence shortly.

(v) Histologic and molecular analysis of mouse tissues, as they become available.

Tissues from the completed mouse studies indicated above have been processed, embedded and sectioned for H&E and immunohistochemical analyses. Analyses to-date have localized tumor cells overexpressing IL6R to myeloid cells in the omentum. The intricate association between these cell types appears to be highly relevant to early metastases of ovarian cancer and is being further explored.

(vi) Preparation of manuscripts.

This task is currently underway to publish the data on the mouse studies of tumor:stromal relationship. The final study of reconstituting soluble gp130 and IL6R will be prepared for publication when the results become available.

KEY RESEARCH ACCOMPLISHMENTS:

- Identification of IL6R in ovarian tumor microenvironment
- Demonstration that differentially-spliced isoform of IL6R is prominent in ovarian cancer
- Host expression of IL6R contributes to the total amount of IL6R present in the tumor microenviroment
- Finding that IL6R expression enhances the earliest metastases of ovarian cancer
- Myeloid cell expression of IL6R is critical to influencing early tumor adhesion to the omentum

REPORTABLE OUTCOMES: Provide a list of reportable outcomes that have resulted from this research to include:

Cell lines: human ovarian carcinoma cells (ES-2 and Skov-3) overexpressing IL6R and with knockdown expression of IL6R and control vector.

Gene-targeted animals: $IL6R^{-/-}$, $IL6R^{fl/fl}$, $LysMCre^{+}/IL\text{-}6R^{fl/fl}$, $AlbCre^{+}/IL\text{-}6R^{fl/fl}$.

Research opportunities provided for individuals based on studies in this award:

Post-doctoral Candidates:	Molly McFarland-Mancini, 2006-2009
	Premkumar Vummidi Giridhar 2009- 2010.
Medical residents:	Kellie Rath, Oct 2008 – Dec 2009

Manuscripts published:

1. Rath, K., Funk, H.M., Bowling, M.C., Richards, W.E., Drew, A.F. (2010) Expression of Soluble Interleukin-6 Receptor in Malignant Ovarian Tissue. Am. J. Obstet. Gynecol. 203(3).e1-8.
2. McFarland, M.M., Funk, H.M., Paluch, A.M., Zhou, M., Vummidi Giridhar, P., Mercer, C.A., Kozma, S.C., Drew, A.F. (2010) Differences in Wound Healing in Mice with Deficiency of Interleukin-6 versus Interleukin-6 Receptor. J. Immunol. 184(12): 7219-28.

CONCLUSION:

Our studies have so far demonstrated that IL6R is present in the ovarian tumor microenvionment and that the differentially-spliced isoform is greatly upregulated compared with normal tissues. This provides one mechanism by IL6R expression is increased in the tumor microenvironment. Host IL6R expression is another means by which this occurs. Overexpression of either tumor or host expression of IL6R in xenograft models influences the earliest steps in ovarian tumor metastasis. The remainder of our studies are designed to elucidate the mechanism by which IL6R isoforms carry out this function. This will have the result of providing opportunities to specifically target IL6R and prevent the earliest steps in ovarian cancer metastasis. Metastasis is the most lethal step in the progression of ovarian cancer.

REFERENCES:

1. K. S. Rath, H. M. Funk, M. C. Bowling, W. E. Richards, A. F. Drew, *Am J Obstet Gynecol* **203**, 230.e1 (sep 2010, 2010).
2. R. M. McLoughlin *et al.*, *J Immunol* **172**, 5676 (May 1, 2004).
3. M. M. McFarland-Mancini *et al.*, *J Immunol* **184**, 7219 (May 10, 2010).
4. C. P. Carmignani, T. A. Sugarbaker, C. M. Bromley, P. H. Sugarbaker, *Cancer Metastasis Rev* **22**, 465 (Dec, 2003).
5. S. M. Khan *et al.*, *Clin Exp Metastasis* **27**, 185 (Mar, 2010).

ONCOLOGY

Expression of soluble interleukin-6 receptor in malignant ovarian tissue

Kellie S. Rath, MD; Holly M. Funk, BSc; Marcia C. Bowling, MD; William E. Richards, MD; Angela F. Drew, PhD

OBJECTIVE: The objective of the study was to investigate interleukin-6 receptor (IL6R) isoforms and sheddases in the ovarian tumor microenvironment.

STUDY DESIGN: Expression of IL6R and sheddases was measured in tissue samples of papillary serous ovarian carcinomas and benign ovaries by real-time polymerase chain reaction and immunohistochemistry. Murine xenograft samples were tested by enzyme-linked immunosorbent assay to discriminate and evaluate tumor and host contributions of IL6R.

RESULTS: IL6R expression was increased in malignant ovarian tumors and localized to epithelial cells. Expression of a soluble splice variant of IL6R was increased in malignant tumors, as were the sheddases for the full-length isoform. An in vivo xenograft model showed that host IL6R expression is also increased and regulated by tumor-associated inflammation.

CONCLUSION: IL6R is overexpressed in epithelial ovarian malignancies because of increases in a soluble IL6R variant, in the sheddases for full-length IL6R and host IL6R expression. Soluble IL6R may be an efficacious target for reducing IL6-mediated ovarian tumor progression.

Key words: a disintegrin and metalloprotease domain 10, a disintegrin and metalloprotease domain 17, cytokine receptor, inflammation, interleukin-6, ovarian tumor

Cite this article as: Rath KS, Funk HM, Bowling MC, et al. Expression of soluble interleukin-6 receptor in malignant ovarian tissue. Am J Obstet Gynecol 2010;203:xx-xx.

Ovarian cancer is the most deadly of the gynecological malignancies.[1] Most gynecologic oncologists initially treat the disease with debulking surgery, followed by adjuvant chemotherapy with platinum and taxane agents. After an initial response to chemotherapy, the cancer will recur in the majority of patients but with chemoresistant properties. The efficacy of second-line and salvage therapies for patients who fail initial surgical and medical therapy is limited at best. A greater understanding of the mechanisms by which ovarian cancers metastasize and develop chemoresistance is essential for reducing the high mortality associated with these malignancies.

Interleukin-6 (IL-6) is an important proinflammatory cytokine that is frequently up-regulated in acute and chronic inflammatory conditions, including many cancers (reviewed elsewhere[2]). IL-6 signaling occurs through a hexameric complex of IL-6, a specific α receptor (IL6R; glycoprotein [gp]80), and a shared β-signaling receptor (gp130).[3] Dimerization of gp130 leads to activation of Janus tyrosine kinases and subsequent translocation of signal transducer and activator of transcription (Stat) transcription factors.[4] Stat3 is the major Stat induced by IL-6 signaling, and its nuclear translocation induces a transcriptional program resulting in inflammation, cell survival, or differentiation, depending on the cellular context.[5,6] In addition to membrane-bound IL6R, several soluble isoforms also exist.[7]

Expression of both membrane-bound and soluble forms of IL6R are largely restricted to hepatocytes and immune cells, and therefore, signaling through membrane-bound IL6R is restricted to these cells. However, the soluble isoforms of IL6R are excreted from these cells types and unexpectedly function as agonists for IL6R signaling and hence allow IL6R-mediated signaling in cells that do not express IL6R. This occurs through initial binding of IL-6 to soluble extracellular IL6R and subsequent binding of this complex to the membrane-bound signaling receptor, gp130.

This binding results in dimerization of gp130, which, in turn, leads to stat3 activation that occurs in a similar fashion to that induced by membrane-bound IL6R. Because gp130 is ubiquitously expressed, the potential to respond to IL-6 is conferred on all cells in the presence of soluble IL6R. This process, known as trans-signaling,[8] has been found to be important in multiple disease states including rheumatoid arthritis, asthma, inflammatory bowel disease, and colon cancer.[9-11] It has been shown that many of the inflammatory functions of IL-6 signaling can be prevented by inhibiting the soluble isoform of IL6R with a solu-

From the Department of Cancer and Cell Biology (Drs Rath and Drew and Ms Funk) and the Division of Gynecologic Oncology, Department of Obstetrics and Gynecology (Drs Rath and Richards), University of Cincinnati School of Medicine, and the Department of Obstetrics and Gynecology (Dr Bowling), Christ Hospital, Cincinnati, OH.

Received Dec. 22, 2009; revised Jan. 29, 2009; accepted March 18, 2010.

Reprints: Angela F. Drew, PhD, Department of Cancer and Cell Biology, Vontz Center for Molecular Studies, University of Cincinnati, 3125 Eden Ave., Cincinnati, OH 45267-0521. angela.drew@uc.edu.

This study was supported in part by the American Cancer Society Grant RSG-06-141-01-CSM (to A.F.D.) and the Department of the Army, Department of Defense Ovarian Cancer Research Program grant (OC080273) (to A.F.D.).

0002-9378/$36.00

doi: 10.1016/j.ajog.2010.03.034

TABLE 1
Patient characteristics

Patient no.	Age	Pathology	Stage
1-16	39-71	Normal ovarian tissue	
17	69	Mixed papillary serous and undifferentiated tumor	IV
18	56	Papillary serous	II
19	62	Papillary serous	IIIC
20	47	Papillary serous	IIIC
21	75	Papillary serous	IIIC
22	50	Papillary serous	IV
23	39	Papillary serous, high grade	IIIC
24	36	Papillary serous cystadenocarcinoma	IB
25	68	Papillary serous	III
26	77	Papillary serous	IV
27	55	Papillary serous	III

Rath. IL-6 receptor in ovarian tumors. Am J Obstet Gynecol 2010.

ble form of gp130.[12] Therefore, the soluble isoform plays important roles in inflammatory contexts by allowing a heightened response to IL-6 in all cell types at the site of inflammatory challenge.

Soluble IL6R can be generated by 2 distinct processes: differential splicing and proteolytic cleavage.[13-15] The differentially spliced isoform lacks a transmembrane domain and is secreted as a soluble, functional receptor.[16] The proteolytic enzymes responsible for cleavage of full-length IL6R are a disintegrin and metalloprotease domain (ADAM)-17, also known as tumor necrosis factor alpha–converting enzyme and to a lesser extent, ADAM10.[17-19] These sheddases cleave full-length IL6R in a membrane proximal site to release a soluble, functional receptor. A study of IL-6 signaling in an angiotensin-induced cardiac model suggested that the 2 forms of soluble IL6R may have different functions leading to either hypertrophy or hypertension.[20]

It is well established that IL-6 is upregulated in both the serum and ascites of ovarian cancer patients and is associated with disease progression.[21-23] IL-6 has also been implicated in chemotherapeutic resistance in ovarian cancer cell lines and in patients with ovarian cancer.[22,24,25] However, the status of IL6R expression in ovarian cancer has not been adequately addressed to date. One study reports increased expression of soluble IL6R in the sera of patients in the early stages of various tumor types, but specific data for ovarian cancer were not available.[26] Despite the importance of the soluble isoforms of IL6R in inflammation, there has not been a characterization of these isoforms in ovarian cancer.

Given that we have previously shown that inflammation drives the spread of ovarian tumors in murine models,[27] a thorough evaluation of inflammatory IL6R isoforms in the tumor microenvironment is needed. Here we describe the increased expression of IL-6, total IL6R, differentially spliced IL6R, ADAM10, and ADAM17 in ovarian tumors. Furthermore, we show that both tumor and host cells contribute to soluble IL6R expression in the tumor environment.

Materials and Methods

Patient tissue collection and cell lines

Tissue samples from malignant and nonmalignant ovaries were collected from patients undergoing routine gynecologic procedures at the University Hospital and the Christ Hospital in Cincinnati, OH (Table 1). Normal ovarian tissue was collected from patients 1-16. Malignant tissue collected from patients 17-27 were from primary ovarian epithelial carcinomas. Tissues were immediately snap frozen in liquid nitrogen at the time of surgery and stored at −80°C until analysis. Human ES-2 and SKOV3, clear cell and serous papillary ovarian carcinoma cell lines, respectively, were obtained from American Type Culture Collection (Manassas, VA). Cells were maintained in Dulbecco's Modified Eagles media with 10%

TABLE 2
Primers used in RT-PCR analysis

Gene	5'	3'
IL-6	CTCACCTCTTCAGAACGAATTGACAAACAAA	GGTACTCTAGGTATACCTCAAACTCCAAAA
IL6R	GCTGTGCTCTTGGTGAGGAAGTTT	CTGAGCTCAAACCGTAGTCTGTAGAAA
IL6R variant 1 (full-length)	GCCTCCCAGTGCAAGATTCTTCTT	CCGCAGCTTCCACGTCTTCTT
IL6R variant 2 (differentially spliced)	GCGACAAGCCTCCCAGGTT	CCGCAGCTTCCACGTCTTCTT
ADAM10	AATGGATTGTGGCTCATTGGTGGG	TGGAAGTGGTTTAGGAGGAGGCAA
ADAM17	CTTATGTTGGCTCTCCCAGAGCAAA	CATCCGGATCATGTTCTGCTCCAAAA

Rath. IL-6 receptor in ovarian tumors. Am J Obstet Gynecol 2010.

fetal calf serum and tested negative for mycoplasma contamination.

Animal studies

Human tumor cell lines (ES-2 and SKOV3) were harvested, resuspended in Matrigel (basement membrane protein gel, BD Biosciences, Franklin Lakes, NJ), and implanted in the ovaries of severe combined immunodeficiency (SCID) mice (Charles River Laboratories, Wilmington, MA), as previously described.[27] Groups of mice (n = 6) were administered acetyl salicylic acid (ASA; 100 mg/kg; Sigma, St Louis, MO), phosphate-buffered saline, or thioglycolate (0.5 mL of a 3% solution; Fluka, Buchs, Switzerland) by twice-weekly intraperitoneal injection. Additional mice without tumors were administered ASA, saline, or thioglycolate. Peritoneal lavage with phosphate-buffered saline was performed on anesthetized mice. Lavage fluid was centrifuged and stored at −80°C until analysis. Guidelines for the care and use of laboratory animals approved by the University of Cincinnati Institutional Animal Care and Use Committee were followed.

RNA isolation and reverse transcription–polymerase chain reaction (RT-PCR)

Ribonucleic acid (RNA) was extracted from patient tissue samples with the RNeasy lipid kit (Qiagen, Valencia, CA) and quantified with a spectrophotometer (Nanodrop, Wilmington, DE). Reverse transcription was performed with the Thermoscript II kit (Invitrogen, Carlsbad, CA). Real-time polymerase chain reaction (PCR) was performed with primers specific for IL-6, both isoforms of IL6R (total IL6R), full-length IL6R (variant 1), differentially spliced IL6R (variant 2), ADAM10, and ADAM17 (Table 2) with a Realplex Mastercycler (Eppendorf, Netheler, Germany). Primer specificity was confirmed by checking product sizes on an agarose gel and performing a melt-curve analysis on each run. Gene expression was normalized against the human L32 housekeeping gene, as previously described.[28]

FIGURE 1
Increased expression of IL-6 and IL6R in malignant ovarian tumors

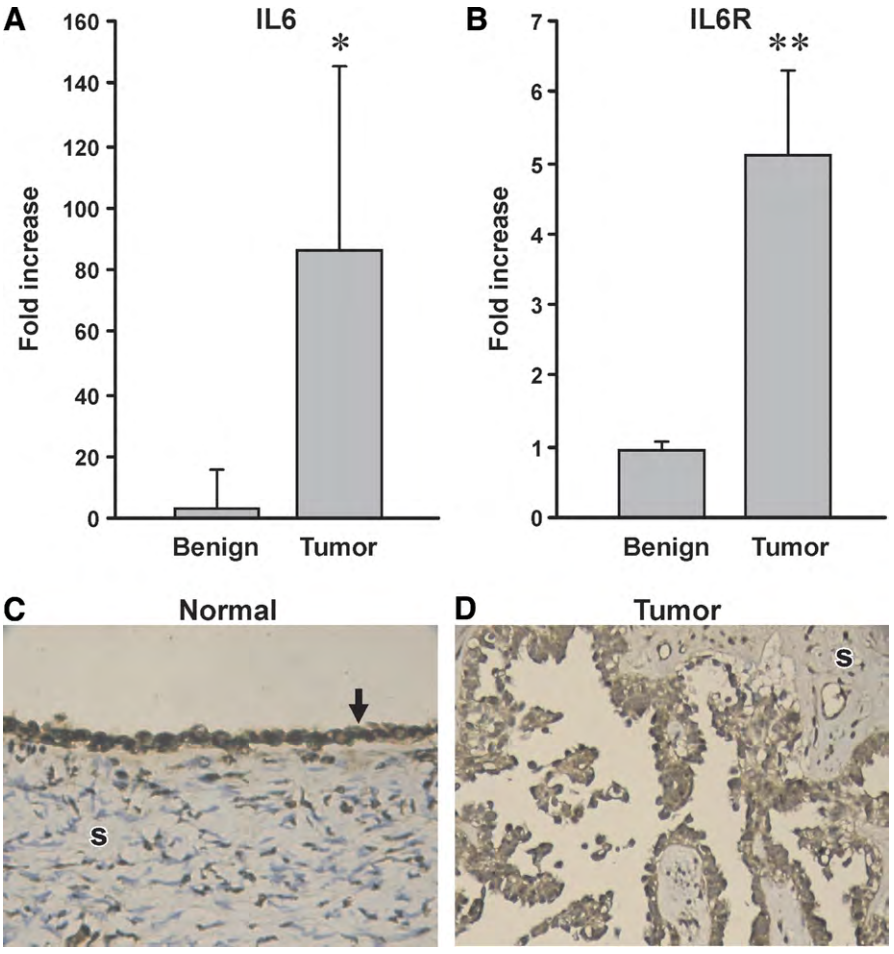

RNA was extracted from ovarian samples from patients with benign gynecologic conditions or ovarian malignancies and assessed for **A,** IL-6 or **B,** total IL6R by quantitative RT-PCR. *Asterisk* indicates $P < .05$; *double asterisk* indicates $P < .001$. Immunohistochemical analysis of ovaries from patients with **C,** no malignancy or **D,** malignant tumors demonstrated intense IL6R positivity in the surface epithelium (*arrow*) and tumor cells but not the stroma (indicated as *s*). Original magnification for **C** and **D**: ×200.

IL-6, interleukin-6; *IL6R*, interleukin-6 receptor; *RT-PCR*, reverse transcription–polymerase chain reaction.

Rath. IL-6 receptor in ovarian tumors. Am J Obstet Gynecol 2010.

Immunohistochemistry

Immunohistochemistry was performed on paraffin-embedded samples of both benign and malignant ovarian tissue to detect IL6R. Briefly, samples were deparaffinized, and antigen retrieval was performed in citrate buffer (10 mM with 0.05% Tween 20, pH 6.0) for 10 minutes at 95°C. Slides were incubated overnight with rabbit antihuman IL6R (sc-661; detects both isoforms) at a dilution of 1:400 at 4°C, followed by biotinylated goat antirabbit immunoglobulin G (1:200). ABC Elite kit (Vector, Burlingame, CA) and 3,3 diaminobenzidine substrate (Sigma) were used in the detection, followed by hematoxylin counterstain.

IL6R ELISA

Peritoneal lavage fluid from mice was analyzed by enzyme-linked immunosorbent assay (ELISA) (R&D Systems, Minneapolis, MN), according to the manufacturer's instructions, to assess expression of human and murine soluble IL6R. Cross-reactivity between human

FIGURE 2
Differentially spliced variant of IL6R

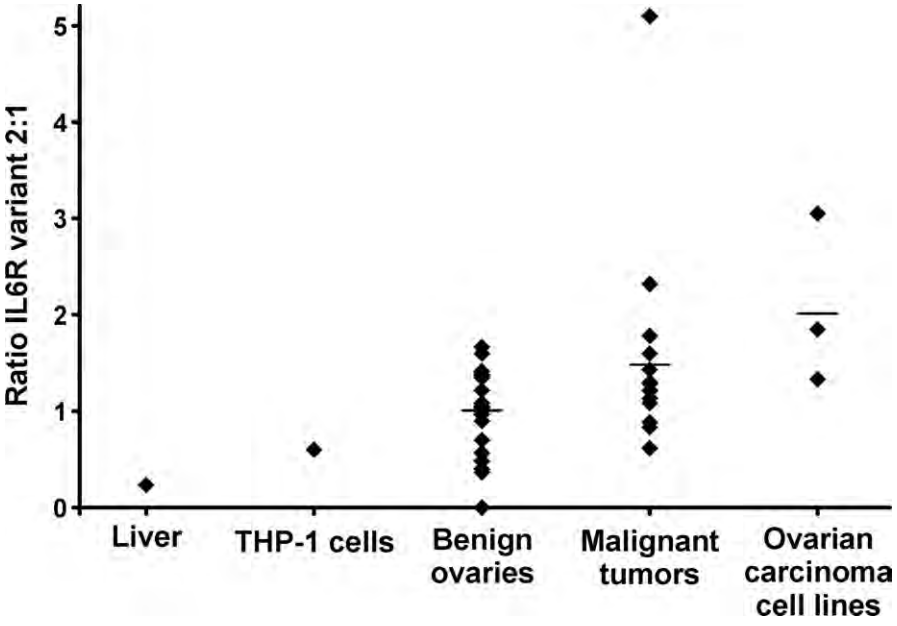

Expression of the differentially spliced variant of IL6R is preferentially increased in malignant ovarian tumors and ovarian carcinoma cell lines compared with benign ovaries, human liver, or the THP-1 monocytic cell line. Data indicate the ratio of differentially spliced IL6R mRNA compared with full-length IL6R mRNA, normalized to normal ovaries. Each data point represents one patient. $P < .05$ for benign ovaries vs malignant tumors or cell lines.

IL6R, interleukin-6 receptor; *mRNA*, messenger RNA.

Rath. IL-6 receptor in ovarian tumors. Am J Obstet Gynecol 2010.

and mouse IL6R is negligible with the use of these species-specific IL6R ELISA kits. The enzymatic reactions were detected at 570 nm and subtracted from background at 450 nm with a spectrophotometric plate reader.

Statistical methods

Data are represented as mean ± SEM were analyzed by the Mann-Whitney *U* test.

RESULTS

Twenty-seven patient samples were collected: 16 with benign ovarian pathology and 11 with ovarian carcinoma (Table 1). Patient age ranges were not significantly different for benign ovary samples (39–71 years; average, 49.1 years) and malignant tumor samples (36–77 years; median, 59.5 years). All tumors were papillary serous and predominantly stage IIIC according to International Federation of Gynecology and Obstetrics classification.

To quantify the production of IL-6 and IL6R in benign ovaries and malignant ovarian tumors, we assessed RNA expression by real-time PCR. We found dramatic up-regulation of IL-6 in malignant ovaries compared with benign ovaries (Figure 1, A), consistent with previous reports.[21-23] Expression of IL6R was also found to be up-regulated in ovarian malignancies (Figure 1, B).

We next sought to identify, by immunohistochemistry, the cell types responsible for IL6R expression in normal and malignant ovarian tissue. IL6R was predominantly expressed in the epithelium of normal ovaries and only minimally in the stroma (Figure 1, C). In serous papillary tumors, IL6R expression was strong in tumor cells and negligible in the tumor stroma (Figure 1, D). Ovarian IL6R expression was therefore a function of both normal and malignant epithelium.

Given the markedly higher proportion of cells expressing IL6R in malignant ovaries, it would be reasonable to expect that the difference in messenger RNA (mRNA) expression levels between normal and malignant tissue would be even greater. This apparent underrepresentation by quantitative PCR could be due to differences in transcriptional or translational efficiencies or to soluble IL6R protein localizing to malignant ovaries despite being produced elsewhere.

Soluble IL6R is known to be important in many inflammatory contexts.[9] To determine whether malignant ovarian tumors were predominantly expressing the full-length (variant 1) or the differentially spliced isoform that lacks the transmembrane domain (variant 2), we used real-time PCR with primers specific for each isoform. Interestingly, we found that the ratio of variant 2 relative to variant 1 was higher in malignant tumor samples than in a human monocytic cell line, normal liver, or benign ovarian samples (Figure 2).

IL6R expression is largely restricted to hepatocytes and immune cells (and some tumor cells); however, expression of soluble IL6R at sites of inflammation, tumors, or both allows IL-6 signaling in other cell types. To determine whether soluble host IL6R expression contributes to the increase in IL6R in the context of an ovarian cancer in vivo, we used a murine xenograft model. Human ovarian carcinoma cell lines were implanted orthotopically into the ovaries of immune-compromised SCID mice.

We implanted cell lines positive (SKOV3) and negative (ES2) for IL6R expression. The rate of tumor formation by SKOV3 cells implanted in the ovary was approximately 50%. Human IL6R was detected in mice in which SKOV3 cell tumors developed but not in ovaries in which tumors did not develop or in ES-2 cell-derived tumors (100% take rate), indicating the specificity of the ELISA (Figure 3, A). Mice that developed ovarian carcinoma had elevated levels of host (mouse) peritoneal soluble IL6R when compared with mice that did not develop carcinoma (Figure 3, B). Tumor

development was identified by gross analysis at necropsy and confirmed by histological analysis (data not shown).

To determine the role of inflammation in host IL6R expression in ovarian tumors, mice were treated with ASA to suppress inflammation, thioglycollate to increase inflammation, or phosphate-buffered saline (vehicle control) during tumor progression. Soluble levels of mouse IL6R were highest in mice treated with thioglycollate and lowest in mice treated with ASA (Figure 4, A).

This pattern of expression closely paralleled that of tumor burden in the mice, as assessed by ascite development and percentage of the diaphragm covered with tumor (Figure 4, B and *inset*). Mice that received inflammation-modulating drugs but that were not implanted with tumor cells expressed only baseline levels of IL6R (Figure 4, A). These data indicate that the increased expression of host soluble IL6R expression was a direct result of the presence of tumor in the peritoneum but was also influenced by the degree of inflammation.

Finally, we evaluated the expression of the 2 known physiological sheddases for full-length IL6R, ADAM17, and ADAM10. We found that the expression of ADAM17 and ADAM10 was increased in malignant ovaries, as compared with benign tissue (Figure 5). The dramatic local increase in expression of these proteases in malignant ovarian tumors provides another mechanism by which soluble IL6R can be generated in the tumor microenvironment.

COMMENT

IL6R plays numerous roles in inflammatory responses and tumor progression.[2,29] In this study, we found that IL6R is expressed in normal and malignant epithelium. We have demonstrated several mechanisms by which increased levels of soluble IL6R occur in the tumor microenvironment, including increased expression of a differentially spliced soluble isoform, up-regulation of sheddases for the membrane-bound form, and increased host expression of soluble IL6R. The increase of IL6R facilitates enhanced responsiveness to IL-6 in ovarian malig-

FIGURE 3
Soluble IL6R protein in mice with human ovarian tumor xenografts

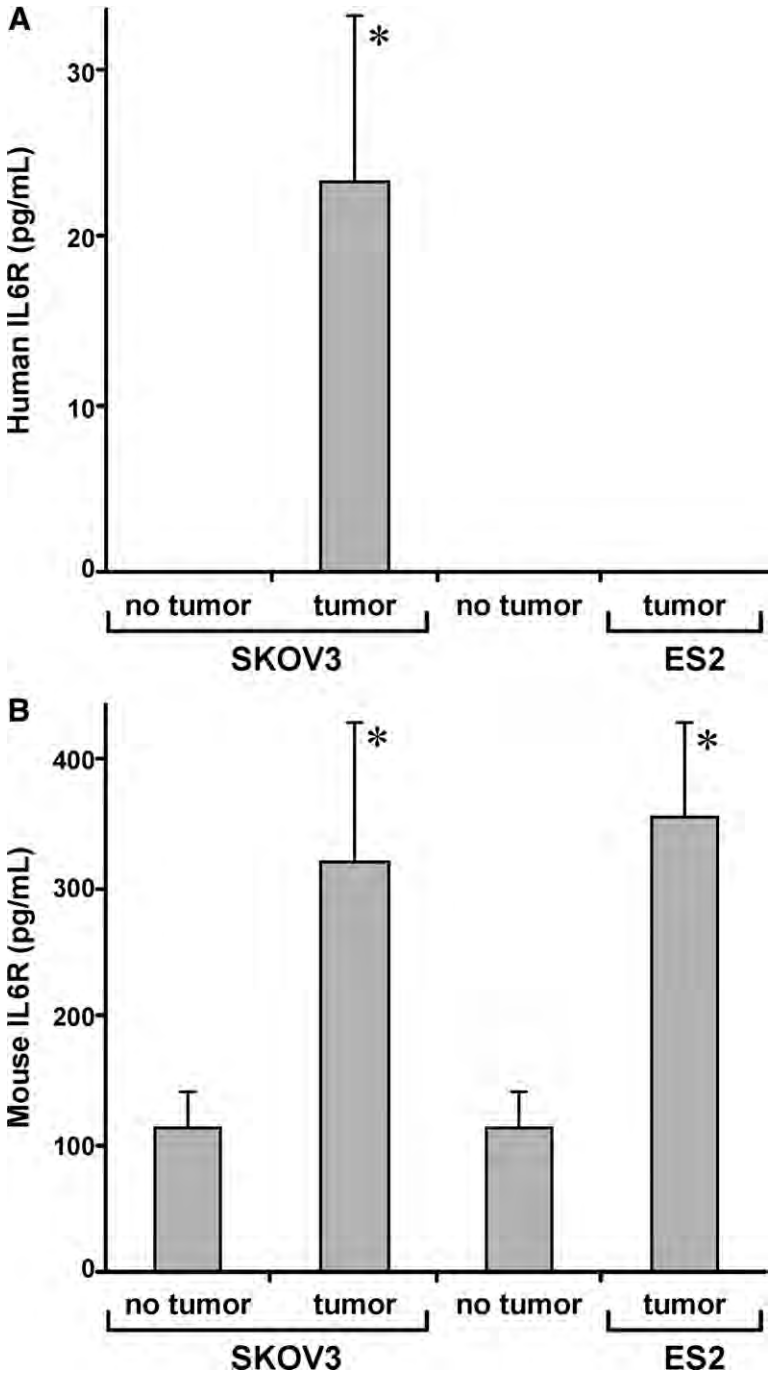

Increased expression of mouse and human soluble IL-6R protein in mice with human ovarian tumor xenografts. **A,** Expression of human sIL6R was increased in the peritoneal lavage fluid of mice that developed human SKOV3 carcinomas, as compared with mice in which tumors did not develop ($P <$ .025). No human IL6R was detected in untreated mice or mice implanted with human ES-2 tumor cells, indicative of the lack of IL6R expression by this tumor cell line. **B,** Baseline levels of mouse IL6R were detected in the peritoneal lavage fluid of untreated mice and mice in which SKOV3 tumors failed to develop. Markedly increased levels of mouse IL6R occurred in mice with either human carcinoma cell line. *Asterisk* indicates $P < .05$.

IL6R, interleukin-6 receptor; *sIL6R*, soluble IL-6R.

Rath. IL-6 receptor in ovarian tumors. Am J Obstet Gynecol 2010.

FIGURE 4
IL6R expression is influenced by mediators of inflammation during tumor progression

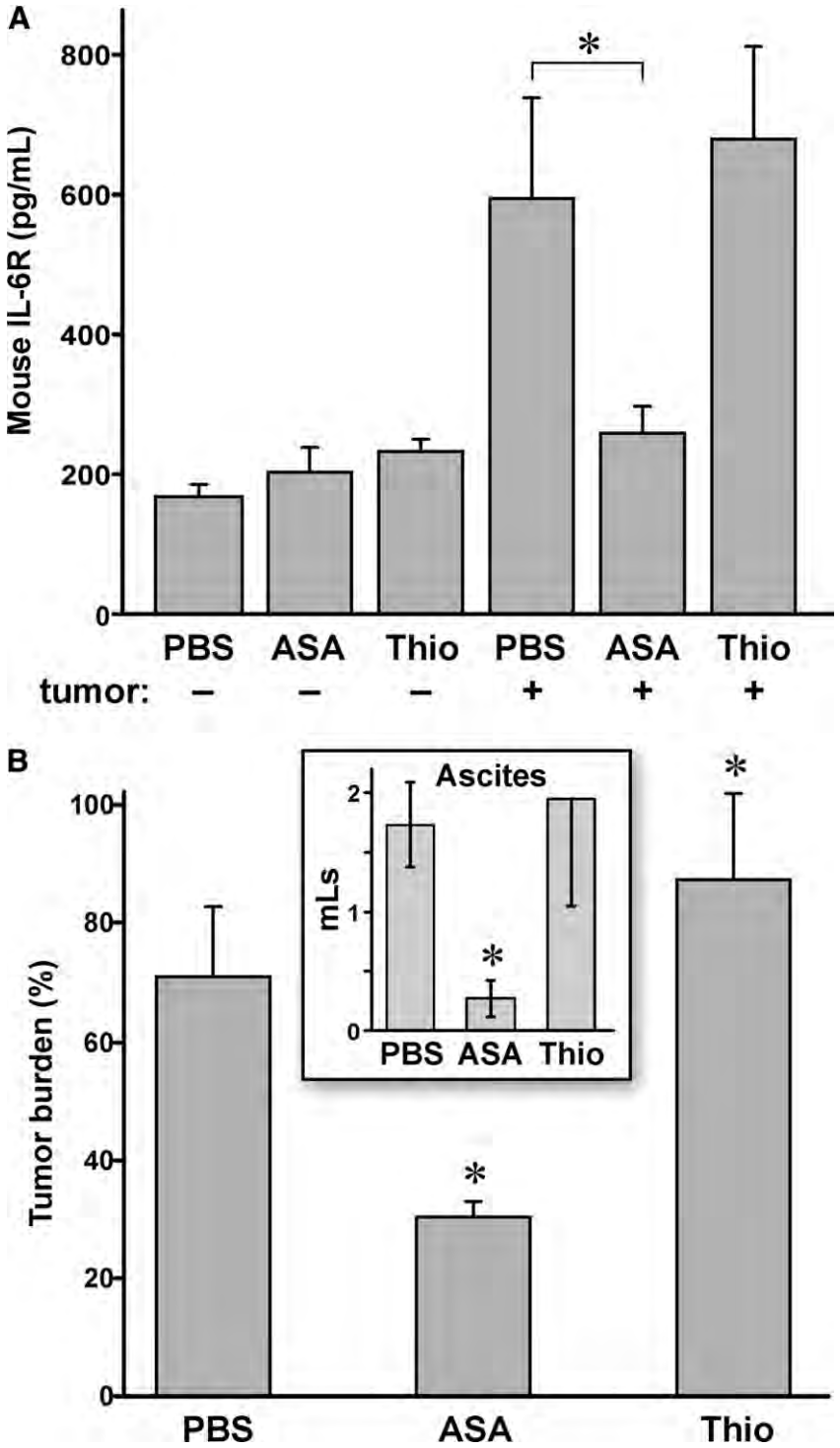

A, Suppressing inflammation with ASA during tumor progression significantly reduced host (mouse) IL6R expression ($P < .05$). Augmenting inflammation with thioglycollate showed a trend toward increased mouse IL6R expression. **B,** The pattern of IL6R expression during inflammation modulation closely resembled that of ascites production (*inset*) and tumor burden. *Asterisk* indicates $P < .05$.

ASA, acetyl salicylic acid; *IL6R*, interleukin-6 receptor.

Rath. IL-6 receptor in ovarian tumors. Am J Obstet Gynecol 2010.

nancies, contributing to increased phosphorylation of Stat3 and up-regulation of cell-survival pathways.[24,30,31]

With no inherent kinase activity, IL6R functions to recognize its specific ligand and to induce dimerization of gp130, the signaling component of the complex. IL6R carries out this role in either soluble or membrane-bound forms; thus, the soluble receptor is effectively an agonist for IL-6 signaling. In fact, blocking only the soluble form of IL6R with exogenous soluble gp130 prevents many, if not all, of the known functions of IL-6 in inflammatory contexts.[11,12]

In the current study, we demonstrate that tumor cells preferentially express a differentially spliced isoform of IL-6R that lacks the transmembrane domain. Expression of this soluble differentially spliced isoform has previously been reported in a subset of monocytes and in several carcinoma cell lines.[32] In addition, our findings suggest that soluble IL6R may also be generated in malignant ovaries by cleavage of the membrane-bound form by increased levels of ADAM10 and ADAM17 proteases. Production of soluble IL6R in ovarian tumor cells may serve to increase IL-6 responsiveness in surrounding tumor cells, stromal cells, or peritoneal mesothelial cells.

Little has been learned about the contribution of the stroma to the expression of IL6R within the context of a tumor, owing to the difficulty in identifying the source of soluble IL6R. Here we have utilized a xenograft model and species-specific ELISAs to allow the distinction between tumor (human) and host (murine) IL6R.

Our data show that, in addition to tumor cell production of IL6R, host cells make a significant contribution to the increased expression of soluble IL6R in the peritoneal environment and that IL6R levels reflect the degree of peritoneal inflammation. It was not possible to determine whether host-derived IL6R is the differentially spliced isoform because this variant is lacking in mice. It is tempting to speculate that immune cells are a predominant source of host IL6R because they are abundant in the ascites

FIGURE 5
Increased expression of ADAM17 and ADAM10 in malignant ovarian tumor tissue

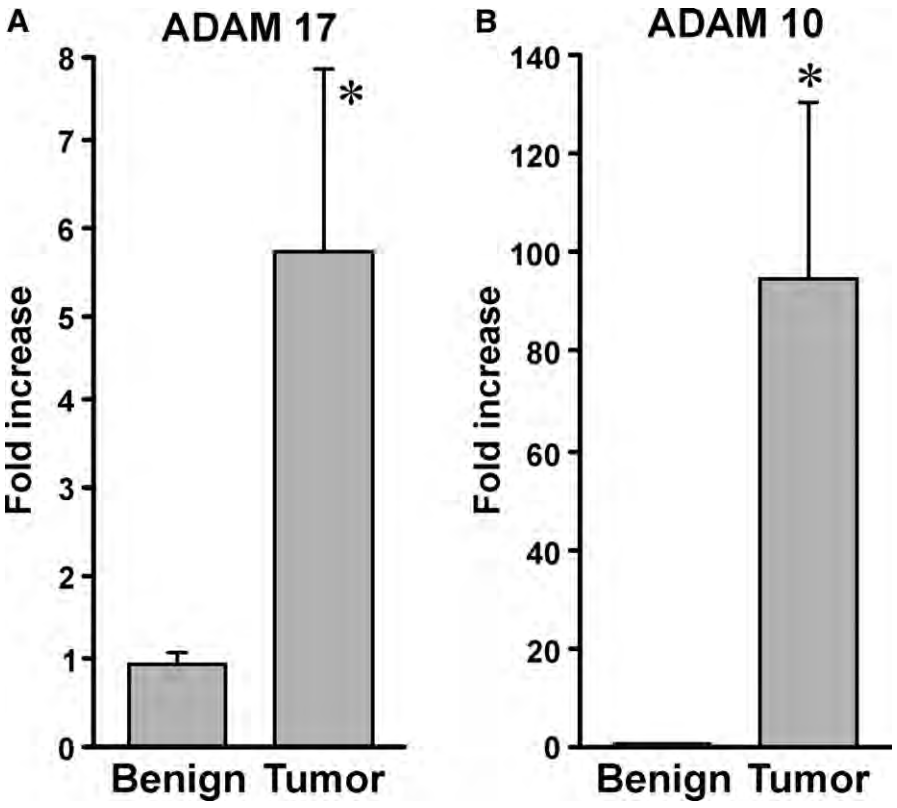

Expression of **A,** mRNA for ADAM17 and **B,** ADAM10 were increased in the ovaries of patients with ovarian cancer compared with benign ovaries. *Asterisk* indicates $P < .001$.

ADAM10, a disintegrin and metalloprotease domain 10; *ADAM17*, a disintegrin and metalloprotease domain 17; *mRNA*, messenger RNA.

Rath. IL-6 receptor in ovarian tumors. Am J Obstet Gynecol 2010.

fluid[33-35] and are known to be a source of shed IL6R in inflammatory contexts.[36]

Given the importance of IL-6 signaling in inflammation, tumor growth, differentiation, and chemoresistance, the identification of IL6R isoforms in malignant ovarian tumors may provide novel therapeutic opportunities. Here we show that expression of soluble isoforms of IL6R is increased by multiple mechanisms, including preferential production of a differentially spliced variant, increased production of sheddases for membrane-bound IL6R, and up-regulation of host inflammation-induced soluble IL6R in the tumor microenvironment. Together these data suggest that trans-signaling through IL6R is a feature of ovarian tumors and that targeting IL6R may provide a novel treatment to decrease the morbidity and mortality of this disease. ■

ACKNOWLEDGMENT

We gratefully acknowledge the assistance of Karen Winstead of the University of Cincinnati Tumor Bank, Dr Maryellen Daston for document editing, and Glenn Doerman for graphical assistance.

REFERENCES

1. American Cancer Society. Cancer facts and figures; 2008. Available at: www.cancer.org/downloads/STT/2008CAFFfinalsecured.pdf. Accessed May 5, 2010.

2. Hong DS, Angelo LS, Kurzrock R. Interleukin-6 and its receptor in cancer: implications for translational therapeutics. Cancer 2007;110:1911-28.

3. Taga T, Hibi M, Hirata Y, et al. Interleukin-6 triggers the association of its receptor with a possible signal transducer, gp130. Cell 1989;58:573-81.

4. Stahl N, Farruggella TJ, Boulton TG, Zhong Z, Darnell JE Jr, Yancopoulos GD. Choice of STATs and other substrates specified by modular tyrosine-based motifs in cytokine receptors. Science 1995;267:1349-53.

5. Yamanaka Y, Nakajima K, Fukada T, Hibi M, Hirano T. Differentiation and growth arrest signals are generated through the cytoplasmic region of gp130 that is essential for Stat3 activation. EMBO J 1996;15:1557-65.

6. Wegenka UM, Buschmann J, Lutticken C, Heinrich PC, Horn F. Acute-phase response factor, a nuclear factor binding to acute-phase response elements, is rapidly activated by interleukin-6 at the posttranslational level. Mol Cell Biol 1993;13:276-88.

7. Jones SA, Rose-John S. The role of soluble receptors in cytokine biology: the agonistic properties of the sIL-6R/IL-6 complex. Biochim Biophys Acta 2002;1592:251-63.

8. Mackiewicz A, Schooltink H, Heinrich PC, Rose-John S. Complex of soluble human IL-6-receptor/IL-6 up-regulates expression of acute-phase proteins. J Immunol 1992;149:2021-7.

9. Jones SA, Richards PJ, Scheller J, Rose-John S. Review: IL-6 transsignaling: the in vivo consequences. J Interferon Cytokine Res 2005;25:241-53.

10. Becker C, Fantini MC, Schramm C, et al. TGF-beta suppresses tumor progression in colon cancer by inhibition of IL-6 trans-signaling. Immunity 2004;21:491-501.

11. Nowell MA, Richards PJ, Horiuchi S, et al. Soluble IL-6 receptor governs IL-6 activity in experimental arthritis: blockade of arthritis severity by soluble glycoprotein 130. J Immunol 2003;171:3202-9.

12. Rabe B, Chalaris A, May U, et al. Transgenic blockade of Interleukin-6-trans-signaling abrogates inflammation. Blood 2008;111:1021-8.

13. Horiuchi S, Koyanagi Y, Zhou Y, et al. Soluble interleukin-6 receptors released from T cell or granulocyte/macrophage cell lines and human peripheral blood mononuclear cells are generated through an alternative splicing mechanism. Eur J Immunol 1994;24:1945-8.

14. Mullberg J, Schooltink H, Stoyan T, Heinrich PC, Rose-John S. Protein kinase C activity is rate limiting for shedding of the interleukin-6 receptor. Biochem Biophys Res Commun 1992;189:794-800.

15. Thabard W, Barille S, Collette M, et al. Myeloma cells release soluble interleukin-6R-alpha in relation to disease progression by two distinct mechanisms: alternative splicing and proteolytic cleavage. Clin Cancer Res 1999;5:2693-7.

16. Lust JA, Jelinek DF, Donovan KA, et al. Sequence, expression and function of an mRNA encoding a soluble form of the human interleukin-6 receptor (sIL-6R). Curr Top Microbiol Immunol 1995;194:199-206.

17. Jones SA, Novick D, Horiuchi S, Yamamoto N, Szalai AJ, Fuller GM. C-reactive protein: a physiological activator of interleukin 6 receptor shedding. J Exp Med 1999;189:599-604.

18. Marin V, Montero-Julian F, Gres S, Bongrand P, Farnarier C, Kaplanski G. Chemotactic

agents induce IL-6R-alpha shedding from polymorphonuclear cells: involvement of a metalloproteinase of the TNF-alpha-converting enzyme (TACE) type. Eur J Immunol 2002;32: 2965-70.

19. Matthews V, Schuster B, Schutze S, et al. Cellular cholesterol depletion triggers shedding of the human interleukin-6 receptor by ADAM10 and ADAM17 (TACE). J Biol Chem 2003; 278:38829-39.

20. Coles B, Fielding CA, Rose-John S, Scheller J, Jones SA, O'Donnell VB. Classic interleukin-6 receptor signaling and interleukin-6 trans-signaling differentially control angiotensin II-dependent hypertension, cardiac signal transducer and activator of transcription-3 activation, and vascular hypertrophy in vivo. Am J Pathol 2007;171:315-25.

21. Moradi MM, Carson LF, Weinberg B, Haney AF, Twiggs LB, Ramakrishnan S. Serum and ascitic fluid levels of interleukin-1, interleukin-6, and tumor necrosis factor-alpha in patients with ovarian epithelial cancer. Cancer 1993;72: 2433-40.

22. Plante M, Rubin SC, Wong GY, Federici MG, Finstad CL, Gastl GA. Interleukin-6 level in serum and ascites as a prognostic factor in patients with epithelial ovarian cancer. Cancer 1994;73:1882-8.

23. Scambia G, Testa U, Benedetti Panici P, et al. Prognostic significance of interleukin 6 serum levels in patients with ovarian cancer. Br J Cancer 1995;71:354-6.

24. Duan Z, Foster R, Bell DA, et al. Signal transducers and activators of transcription 3 pathway activation in drug-resistant ovarian cancer. Clin Cancer Res 2006;12:5055-63.

25. Penson RT, Kronish K, Duan Z, et al. Cytokines IL-1beta, IL-2, IL-6, IL-8, MCP-1, GM-CSF and TNF-alpha in patients with epithelial ovarian cancer and their relationship to treatment with paclitaxel. Int J Gynecol Cancer 2000;10:33-41.

26. Kovacs E. Investigation of interleukin-6 (IL-6), soluble IL-6 receptor (sIL-6R) and soluble gp130 (sgp130) in sera of cancer patients. Biomed Pharmacother 2001;55:391-6.

27. Robinson-Smith TM, Isaacsohn I, Mercer CA, et al. Macrophages mediate inflammation-enhanced metastasis of ovarian tumors in mice. Cancer Res 2007;67:5708-16.

28. Drew AF, Blick TJ, Lafleur MA, et al. Correlation of tumor- and stromal-derived MT1-MMP expression with progression of human ovarian tumors in SCID mice. Gynecol Oncol 2004; 95:437-48.

29. Nilsson MB, Langley RR, Fidler IJ. Interleukin-6, secreted by human ovarian carcinoma cells, is a potent proangiogenic cytokine. Cancer Res 2005;65:10794-800.

30. Silver DL, Naora H, Liu J, Cheng W, Montell DJ. Activated signal transducer and activator of transcription (STAT) 3: localization in focal adhesions and function in ovarian cancer cell motility. Cancer Res 2004;64:3550-8.

31. Syed V, Ulinski G, Mok SC, Ho SM. Reproductive hormone-induced, STAT3-mediated interleukin 6 action in normal and malignant human ovarian surface epithelial cells. J Natl Cancer Inst 2002;94:617-29.

32. Jones SA, Horiuchi S, Novick D, Yamamoto N, Fuller GM. Shedding of the soluble IL-6 receptor is triggered by Ca2+ mobilization, while basal release is predominantly the product of differential mRNA splicing in THP-1 cells. Eur J Immunol 1998;28:3514-22.

33. Mantovani A, Polentarutti N, Peri G, et al. Cytotoxicity on tumor cells of peripheral blood monocytes and tumor-associated macrophages in patients with ascites ovarian tumors. J Natl Cancer Inst 1980;64:1307-15.

34. Haskill S, Becker S, Fowler W, Walton L. Mononuclear-cell infiltration in ovarian cancer. I. Inflammatory-cell infiltrates from tumour and ascites material. Br J Cancer 1982;45:728-36.

35. Melichar B, Savary CA, Patenia R, Templin S, Melicharova K, Freedman RS. Phenotype and antitumor activity of ascitic fluid monocytes in patients with ovarian carcinoma. Int J Gynecol Cancer 2003;13:435-43.

36. Chalaris A, Rabe B, Paliga K, et al. Apoptosis is a natural stimulus of IL6R shedding and contributes to the proinflammatory trans-signaling function of neutrophils. Blood 2007; 110:1748-55.

The Journal of Immunology

Differences in Wound Healing in Mice with Deficiency of IL-6 versus IL-6 Receptor

Molly M. McFarland-Mancini, Holly M. Funk, Andrew M. Paluch, Mingfu Zhou, Premkumar Vummidi Giridhar, Carol A. Mercer, Sara C. Kozma and Angela F. Drew

J. Immunol. published online May 10, 2010; doi:10.4049/jimmunol.0901929

The Journal of Immunology is published twice each month by The American Association of Immunologists, Inc., 9650 Rockville Pike, Bethesda, MD 20814-3994.

Print ISSN: 0022-1767 Online ISSN: 1550-6606.

Published May 10, 2010, doi:10.4049/jimmunol.0901929

Differences in Wound Healing in Mice with Deficiency of IL-6 versus IL-6 Receptor

Molly M. McFarland-Mancini,*[,1] Holly M. Funk,*[,1] Andrew M. Paluch,* Mingfu Zhou,* Premkumar Vummidi Giridhar,* Carol A. Mercer,[†] Sara C. Kozma,* and Angela F. Drew*

IL-6 modulates immune responses and is essential for timely wound healing. As the functions mediated by IL-6 require binding to its specific receptor, IL-6Rα, it was expected that mice lacking IL-6Rα would have the same phenotype as IL-6–deficient mice. However, although IL-6Rα–deficient mice share many of the inflammatory deficits seen in IL-6–deficient mice, they do not display the delay in wound healing. Surprisingly, mice with a combined deficit of IL-6 and IL-6Rα, or IL-6–deficient mice treated with an IL-6Rα–blocking Ab, showed improved wound healing relative to mice with IL-6 deficiency, indicating that the absence of the receptor contributed to the restoration of timely wound healing, rather than promiscuity of IL-6 with an alternate receptor. Wounds in mice lacking IL-6 showed delays in macrophage infiltration, fibrin clearance, and wound contraction that were not seen in mice lacking IL-6Rα alone and were greatly reduced in mice with a combined deficit of IL-6 and IL-6Rα. MAPK activation-loop phosphorylation was elevated in wounds of IL-6Rα–deficient mice, and treatment of wounds in these mice with the MEK inhibitor U0126 resulted in a delay in wound healing suggesting that aberrant ERK activation may contribute to improved healing. These findings underscore a deeper complexity for IL-6Rα function in inflammation than has been recognized previously. ***The Journal of Immunology*****, 2010, 184: 000–000.**

Interleukin 6 is a pleiotropic cytokine with roles in generating acute phase responses, inflammation, and lymphocyte differentiation. Numerous cell types produce IL-6, especially at sites of inflammation. IL-6 functions are mediated by binding to its specific receptor, IL-6Rα (gp80 and CD126). IL-6Rα is the only known receptor for IL-6, and its expression is predominantly restricted to hepatocytes and immune cells. Recently, ciliary neurotrophic factor (CNTF) and IL-27, two other members of the IL-6 family, have been demonstrated to bind IL-6Rα in vitro but with lower affinity than IL-6, and thus, the in vivo relevance of these findings remains unclear (1, 2). IL-6 engagement of IL-6Rα induces homodimerization of the ubiquitously expressed, common IL-6 family signaling receptor gp130 (IL-6 signaling transducer). Mammalian IL-6, however, cannot directly engage gp130 in the absence of IL-6Rα (3).

IL-6Rα contains an extracellular Ig-like domain, a cytokine receptor homology module, a transmembrane domain, and a nonsignaling intracellular domain. The cytokine receptor homology module is made up of two fibronectin type III domains and is responsible for recognition and binding of IL-6 and gp130 (reviewed in Ref. 4). Typical for a cytokine receptor, IL-6Rα does not possess kinase activity. Ligand-bound IL-6Rα induces dimerization of gp130 (5). The Janus family kinases, JAK1, JAK2, and TYK2, are constitutively associated with the cytoplasmic tail of gp130 and phosphorylate gp130 dimers (6, 7). The transcription factors Stat3 and, to a lesser extent, Stat1 dock at any of four C-terminal tyrosines on gp130 (8, 9). JAKs phosphorylate the Stat proteins inducing Stat dimerization, translocation to the nucleus, and transcription of genes with IL-6–responsive elements (10). IL-6–induced Stat3 activation is negatively regulated by suppressor of cytokine signaling 3 and Src homology region 2 domain-containing phosphatase 2 binding to a membrane-proximal gp130 phospho-tyrosine residue (Y759), resulting in Ras activation and ERK signaling (11–13). Both Stat3 and Erk activation result in cell proliferation, survival, differentiation, and inflammation, and both are frequently upregulated in tumors.

IL-6 signaling can also occur through a soluble form of the receptor that can bind IL-6 and subsequently induce gp130 dimerization (3). This process is known as trans-signaling and allows cells that do not express IL-6Rα to respond to IL-6 (14). Soluble forms of IL-6Rα occur as the result of either of two distinct processes: alternative splicing or proteolytic cleavage (15–17). The importance of each isoform in physiologic processes is not clearly understood. It is known from mice overexpressing human soluble IL-6Rα that the soluble isoform plays a role in sensitizing cells to IL-6 signaling and prolonging IL-6 half-life (18). Inhibition of the soluble form of IL-6Rα in vivo is sufficient to block many of the known functions of IL-6 signaling, such as modulation of the inflammatory response (19, 20). Neutrophil infiltration and apoptosis are early events in the inflammatory response that trigger IL-6Rα shedding and subsequent monocyte infiltration (19–22). Despite high expression of membrane-bound IL-6Rα, human osteoblasts are unable to respond to IL-6 unless the receptor is cleaved to produce the soluble form (23). It has not

*Department of Cancer and Cell Biology, Vontz Center for Molecular Studies, University of Cincinnati, Cincinnati, OH 45267; and [†]PDS Biotechnology, Lawrenceburg, IN 47025

[1]M.M.M.-M. and H.M.F. contributed equally to this work.

Received for publication June 18, 2009. Accepted for publication April 15, 2010.

This work was supported by a grant from the American Cancer Society (RSG-06-141-01; to A.F.D.) and the Department of the Army, Department of Defense Ovarian Cancer Research Program (OC080273; to A.F.D.).

Address correspondence and reprint requests to Dr. Angela F. Drew, Department of Cancer and Cell Biology, Vontz Center for Molecular Studies, University of Cincinnati, 3125 Eden Avenue, Cincinnati, OH 45267-0521. E-mail address: adrew41@gmail.com

Abbreviations used in this paper: Arg1, arginase 1; CNTF, ciliary neurotrophic factor; DIG, digoxigenin; ES, embryonic stem; fbg, fibrinogen; s, soluble; SAA, serum amyloid A; WT, wild-type.

been well established whether any nonredundant function exists for the membrane-bound form of IL-6Rα.

IL-6–deficient ($Il6^{-/-}$) mice were generated ~15 y ago (24, 25). Their multiple phenotypic abnormalities are not surprising, because of the pleiotropic functions ascribed to IL-6. Although $Il6^{-/-}$ mice have no apparent developmental abnormalities, they have an impaired capacity to mount immune responses to several pathogens and to generate acute-phase responses (24). In addition, they have reduced capacity for liver regeneration and develop age-related obesity (26, 27). $Il6^{-/-}$ mice display resistance to experimental autoimmune conditions, such as encephalitis, and protection against bone loss after ovariectomy (25, 28). Studies using experimental tumor models in $Il6^{-/-}$ mice have reported both tumor-protective and tumor-promoting effects for IL-6, depending on the tumor model used (29–31). A better understanding of the functions of IL-6 and its receptor in different contexts may provide opportunities for more effective manipulation of IL-6 signaling in the treatment of inflammation and cancer.

$Il6^{-/-}$ mice display significant defects in wound healing. Wound healing is a tightly regulated process in which platelets and fibrin immediately fill the wound bed with an insoluble clot, and significant neutrophil immigration occurs shortly thereafter (reviewed in Ref. 32). Re-epithelialization proceeds by adjacent keratinocyte proliferation and migration over the wound area. Neutrophils in wounds are important for microbe neutralization, but their absence from sterile wounds does not delay healing (33, 34). Monocyte/macrophages are subsequently recruited and play roles in the clearance of debris and the provision of growth and angiogenic factors. Macrophages in wounds typically express markers indicating alternate activation pathways with functions in tissue remodeling and angiogenesis, rather than classically activated macrophages that function to kill pathogens. Wounds in mice with inhibited macrophage function display excess fibrin and cellular debris and heal more slowly than those in untreated mice (35). Wound healing is delayed in $Il6^{-/-}$ mice as a result of impaired re-epithelialization, angiogenesis, and macrophage infiltration (36, 37).

In this paper, we report on mice with complete and conditional deficiencies of IL-6Rα, which were generated to better understand the relationship between soluble and membrane-bound receptor and to identify any phenotypic discrepancies that may exist, as compared with $Il6^{-/-}$ mice. Although IL-6 and IL-6Rα are believed to be exclusive and essential components of IL-6 signaling in vivo, we report both similarities and differences between the phenotypes of $Il6^{-/-}$ and $Il6ra^{-/-}$ mice. These studies indicate an unanticipated compensatory improvement in wound healing in $Il6ra^{-/-}$ mice but not in $Il6^{-/-}$ mice, which suggests a greater complexity in IL-6Rα function than was previously appreciated.

Materials and Methods

Generation of Il6ra-knockout mice

IL-6ra–deficient mice were generated by the insertion of a targeting vector into the *IL-6ra* genomic locus. The targeting vector included the selection cassette loxP-frt-pMC1neopA-frt in which the neo gene is flanked by frt sites. Murine *IL-6ra* exons 4, 5, and 6 were inserted between the loxP sequences. The construct was introduced into embryonic stem (ES) cells on a C57BL/6 background for homologous recombination. To prevent changes in the level of gene expression in mice carrying the floxed allele, the resulting loxP sites of the recombined allele were located in nonconserved intronic sequences known to share no sequence conservation between mouse and human and to be devoid of transcription factor binding sites. Recombined ES cell clones were identified by PCR, and a successful single insertion was confirmed by Southern blot analysis. Blastocysts containing ES cells with the floxed allele were implanted, and germline mice were bred with EIIa-cre mice on a C57BL/6 background, resulting in the deletion of *IL-6ra* exons 4, 5, and 6 (the cytokine receptor binding module) and the Neo cassette. Further breeding with C57BL/6 mice was carried out to remove the Cre construct, and mice were then bred to homozygosity for the deleted *IL-6ra* allele. Genotypes were confirmed by PCR analysis and Southern blotting. Studies included in this paper have been reviewed and approved by the University of Cincinnati Institutional Animal Care and Use Committee.

Southern blot analysis

Genomic DNA was prepared by phenol/chloroform extraction and digested overnight with restriction enzymes. Samples were loaded onto a 0.8% agarose gel in tris-acetate EDTA buffer and electrophoresed. The gel was stained with ethidium bromide for 10 min in tris-acetate EDTA buffer, imaged by UV, and then transferred overnight in 20× SSC onto a positively charged nylon membrane (Roche, Basel, Switzerland). Digoxigenin (DIG)-labeled probes were prepared using the PCR DIG Probe Synthesis Kit (Roche), according to the manufacturer's instructions. The membrane was hybridized with 50 ng/ml DIG-labeled probe, followed by chemiluminescent detection with anti-DIG alkaline phosphatase Ab and CSPD substrate.

Generation and maintenance of mice with conditional expression of IL-6Rα

Mice with a floxed allele of *IL-6ra* ($Il6ra^{fl/+}$) were first crossed with $FLPe^{+/+}$ mice (38) to delete the FRT-flanked Neo cassette in the targeting vector. Progeny with successful excision of Neo, as determined by PCR, were crossed with mice expressing Cre recombinase under the control of the albumin promoter ($AlbCre^{+}$) (39) or the lysozyme M promoter ($LysM\text{-}Cre^{+}$) (40). Progeny lacking the FLPe allele were selected for further breeding. $Il6ra^{fl/fl}/AlbCre^{+/+}$ mice were maintained as homozygotes for both alleles. $Il6ra^{fl/fl}/LysMCre^{+/-}$ mice used in experiments were bred from colonies of $Il6ra^{fl/fl}$ and $Il6ra^{fl/fl}/LysMCre^{+/+}$ mice. All mouse strains were on a C57BL/6 background.

Genotyping

DNA from ear clippings was isolated by using the SYBR Green Extract-N-Amp Tissue PCR kit (Sigma-Aldrich, St. Louis, MO). Primers for the wild-type (WT) *IL-6ra* allele (5′-CTGGGACCCGAGTTACTACTT-3′ and 5′-CAGCAACACCGTGAACTCCTTT-3′), the floxed *IL-6ra* allele (5′-GCCTGGGTGGAGAGGCTTTTT-3′ and 5′-CCCAGTGAGCTCCACCATCAAA-3′), and the excised *IL-6ra* allele (5′-CTGGGACAGGGAAGGGCTTTT-3′ and 5′-CCCAGTGAGCTCCACCATCAAA-3′) were used in real-time PCR analysis. AlbCre, LysMCre, and FLPe mice were genotyped as per protocols from their originating laboratories (JAX Mice Database, The Jackson Laboratory, Bar Harbor, ME).

Harvesting of normal and inflammatory-challenged tissues

Spleen, liver, and lung tissues were collected from euthanized mice for analysis. Plasma was prepared from EDTA-treated blood collected from the retro-orbital plexus. Hepatocytes were prepared from anesthetized mice by in situ liver perfusion and Percoll gradient separation, as described previously (41). Thioglycolate-elicited macrophages and granulocytes were collected by peritoneal lavage 24 or 48 h after i.p. injection of 3% thioglycolate broth. Cells were incubated on plastic for 1 h to enrich for adherent macrophages. Acute-phase responses were assessed in plasma and livers collected from mice given a s.c. injection of 100 μl turpentine at various intervals prior to sacrifice.

Air-pouch experiments were performed as described previously (20). Briefly, mice were injected s.c. in the center of the back with 6 and 4 ml sterile air at days −6 and −3, respectively, to create an air pouch. Inflammation was elicited at day 0 by injecting 1 ml 1% carrageenan (Sigma-Aldrich) in PBS into the air pouch. Lavage was performed at days 3 and 7 after carrageenan administration. Lavage fluid was spun onto slides with a cytospin (Thermo Shandon, Pittsburgh, PA) and stained with Kwik-Diff (Thermo Shandon). Differential cell counts were performed by a hematologist (C.A.M.) on three to four microscope fields per sample.

Full-thickness excisional wounds were prepared on shaved dorsal skin by 4-mm-punch biopsy (small wounds; Acuderm, Fort Lauderdale, FL) or with a fine-scissor cutting around a 1-cm^2 template (large wounds). Mice were housed individually, and wounds were left undressed. Wounds were photographed and examined daily, and the percentage of wound closure was assessed as the size of the remaining wound area relative to the original template. Wounds were collected after 1, 2, 5, 8, and 11 d for analysis. For MEK inhibition, wounds were treated daily with topical U0126 (10 μg dissolved in 25 μl DMSO; Selleck Chemicals, Houston, TX) or vehicle alone. In other experiments, mice were given daily peritoneal injections of Abs specific for mouse IL-6Rα (500 μg/mouse; BioExpress, West Lebanon, NH), mouse gp130 (7.5 μg/mouse; eBioscience, San Diego, CA), mouse IL-27/p28 (37 μg/mouse; Shenandoah Biotech, Warwick, PA), or rat IgG (Sigma-Aldrich) diluted to a similar concentration in PBS.

Real-time PCR analysis

RNA from WT and *Il6ra*$^{-/-}$ mice was isolated using the Nucleospin II Kit (Macherey-Nagel, Bethlehem, PA). One microgram of mRNA was reverse transcribed with the Thermoscript II Kit (Invitrogen, Carlsbad, CA). Twenty nanograms of cDNA was used for subsequent PCR analysis. Quantitative PCR was performed using the Realplex Mastercycler (Eppendorf) and the following primers: L32 (*Rpl32*) 5′-CTTAGAGGACACGTTGTGAGCAATC-3′ and 5′-GCTGTGCTGCTCTTTCTACAATGGCTTTT-3′; haptoglobin, 5′-TATGGATGCCAAAGGCAGCTTTCC-3′ and 5′-TCGCTGTGGTTCAGGAAGAGGTTT-3′; serum amyloid A (SAA), 5′-AGAGGACATGAGGACACCATTGCT-3′ and 5′-AGGACGCTCAGTATTTGTCAGGCA-3′; and fibrinogen, 5′-GATGAACAAATGTCACGCAGGCCA-3′ and 5′-GCCCAAATAATGCCGTCGTCGAAA-3′. Each analysis was repeated at least twice to ensure reproducibility. To ensure specificity, real-time melt curves were analyzed, and band sizes were checked on agarose gels. Values were normalized against murine L32, housekeeping gene.

Western blotting and ELISA

Protein lysates were prepared from liver and spleen tissue and quantified by protein assay (Bio-Rad DC; Bio-Rad, Hercules, CA) for Western blotting. Reduced samples were electrophoresed on 8% polyacrylamide gels and transferred to polyvinylidene difluoride membranes (Millipore, Bedford, MA). Membranes were blocked in 5% milk for 1 h. Primary Ab dilutions were applied at 4°C overnight at the following dilutions: rabbit anti-mouse IL-6Rα IgG (1/400; Santa Cruz Biotechnology, Santa Cruz, CA), rabbit anti–β-actin (1/1000; Cell Signaling Technology, Beverly, MA), phospho-Stat3 (1/800, Ser^{727}; Cell Signaling Technology), Stat3 (1/1000, C-20; Santa Cruz Biotechnology), phospho-p44/42 MAPK, ERK1/2, and p44/42 MAPK (1/1000, numbers 4370 and 4695; Cell Signaling Technology). Primary Abs were detected with donkey anti-rabbit IgG-HRP (1/10,000; Novus Biologicals, Littleton, CO) and luminol (ECL Plus; PerkinElmer, Wellesley, MA). ELISAs were used to detect murine soluble IL-6Rα (R&D Systems, Minneapolis, MN) and SAA (Invitrogen) in EDTA-treated plasma.

Histology and immunohistochemistry

Wound tissues were collected into Glyofixx fixative (Thermo Shandon) at necropsy and processed into paraffin. A separate group of wounds was fixed in zinc fixative (BD Biosciences, San Jose, CA) for CD31 immunostaining. 4 μm sections were prepared and routinely stained with H&E. Re-epithelialization was assessed by measuring the percentage of the wound area covered with keratinocytes. Immunohistochemistry was performed on dewaxed tissues after Ag retrieval by heating in citrate buffer or EDTA (F4/80). Sections were blocked with 10% serum, 5% BSA in TBS. Primary Abs were used at the following dilutions: F4/80 (1/400; eBioscience), CD31 (BD Biosciences), fibrinogen [1/1000 (42)], and arginase I (1/100; BD Biosciences). Arginase staining was performed with the Mouse-on-Mouse Blocking kit (Vector Laboratories, Burlingame, CA). Endogenous peroxidase was blocked prior to adding biotinylated secondary Abs (1/200; Vector Laboratories). ABC Elite kit (Vector Laboratories) and diaminobenzidine (Sigma-Aldrich), VectorRed (Vector Laboratories), or Fast Red (Sigma-Aldrich) substrates were used. Morphometry was performed by investigators unaware of the genotypes of the mice. Vascular density was assessed by counting luminal structures in three high-power fields per wound. Macrophages were quantified by measuring the percentage of two randomly selected high-power fields within the wound area that were positive for the substrate (VectorRed) above a predetermined threshold (ImageJ software). Fibrin staining was assessed by a pathologist unaware of the mouse genotypes.

Statistics

Statistics were performed by the Mann-Whitney *U* test for pairwise comparisons or the Kruskall-Wallis test for multiple comparisons. Data are expressed as average ± SEM.

Results

Generation of Il6ra$^{-/-}$ *mice*

Mice with a floxed allele of *IL-6ra* (*Il6ra*$^{fl/+}$) were generated by homologous recombination with a vector containing LoxP sites around exons 4–6 and a neomycin cassette (Fig. 1*A*). *Il6ra*$^{fl/+}$ mice were crossed with EIIa-Cre mice, and the offspring were interbred to obtain mice with a complete deficiency of IL-6Rα (EIIa-Cre$^{+/-}$/IL-6Rα$^{-/-}$) (Fig. 1*A*). Southern blotting indicated an absence of the WT 11-kb genomic DNA fragment and the presence of the predicted 9-kb excised allele in mice homozygous for the floxed allele (Fig. 1*B*). Subsequent breeding to remove the Cre-recombinase gene was performed. The absence of mRNA for *IL-6ra* was determined by real-time PCR on liver and lung tissue (Fig. 1*C*). IL-6Rα protein was absent from liver and spleen lysates prepared from *Il6ra*$^{-/-}$ mice and present in WT (*Il6ra*$^{+/+}$) and heterozygous (*Il6ra*$^{+/-}$) mice (Fig. 1*D*). Similarly, soluble IL-6Rα was abundant in *Il6ra*$^{+/+}$ and *Il6ra*$^{+/-}$ mice and undetectable in *Il6ra*$^{-/-}$ mice (Fig. 1*E*). Although the presence of a truncated IL-6Rα protein in *Il6ra*$^{-/-}$ mice cannot be formally excluded, such a product is unlikely because of 1) the presence of an incomplete domain, 2) unpaired cysteine residues because of the deletion of the cytokine homology domain, and 3) the inability of a polyclonal Ab raised against the entire extracellular domain of IL-6Rα to recognize any product in null mice while detecting abundant product in WT mice. *Il6ra*$^{-/-}$ mice were normal in appearance and were born in the expected Mendelian ratio.

Il6ra$^{-/-}$ *mice have a defective response to IL-6*

IL-6 is critical for the acute-phase response to s.c. injected turpentine (43, 44). To assess the response of *Il6ra*$^{-/-}$ mice, groups of mice were s.c. injected with turpentine. Hepatic production of the acute-phase reactants fibrinogen, haptoglobin, and SAA was markedly diminished or absent in *Il6ra*$^{-/-}$ mice, as assessed by real-time PCR (Fig. 2*A*) and by ELISA for SAA (Fig. 2*B*). Similar results were obtained in *Il6*$^{-/-}$ mice (Fig. 2*A*, 2*B*), as reported previously (43). Thus, IL-6 signaling function is abrogated in *Il6ra*$^{-/-}$ mice in the context of generating an acute-phase response.

IL-6 has been shown to be important in the progression of inflammatory responses from a neutrophil-dominant phase to a macrophage-dominant phase (21). To determine whether this is also the case in *Il6ra*$^{-/-}$ mice, we created s.c. air pouches in mice and injected carrageenan as described previously (20). Although the proportion of neutrophils and macrophages in the pouch fluid was not different between the groups 3 d after carrageenan administration, neutrophil resolution was impaired after 7 d (Fig. 2*C*), and macrophage infiltration was delayed (Fig. 2*D*) in both *Il6*$^{-/-}$ and *Il6ra*$^{-/-}$ mice. Given that IL-6Rα is believed to be the exclusive binding partner required to facilitate the interaction with the common IL-6 family receptor gp130, it was not surprising to find that deficiencies of either IL-6 or IL-6Rα induced the same phenotypic abnormalities compared with WT mice.

Hepatocyte production of IL-6Rα is critical for the acute-phase response but myeloid cells secrete most of the circulating IL-6Rα

IL-6Rα expression has been reported to be predominantly restricted to hepatocytes and immune cells. To elucidate the importance of each compartment in IL-6Rα–dependent processes, we generated mice with conditional deficiency of IL-6Rα in either hepatocytes or lysozyme M-expressing cells (macrophages and granulocytes) by crossing *Il6ra*$^{fl/fl}$ mice with mice expressing Cre recombinase under the control of the albumin (AlbCre) or lysozyme M (LysMCre) promoters, respectively. Significant reduction in IL-6Rα expression was observed in hepatocytes of AlbCre$^{+/+}$/*Il6ra*$^{fl/fl}$ mice (Fig. 3*A*) and in thioglycolate-elicited macrophages of LysMCre$^{+/-}$/*Il6ra*$^{fl/fl}$ mice (Fig. 3*B*). Interestingly, expression of soluble IL-6Rα in plasma was more dependent on immune cell secretion than on hepatic production, because LysMCre$^{+/-}$/*Il6ra*$^{fl/fl}$ mice had lower levels of IL-6Rα levels (39.95% of WT) than AlbCre$^{+/+}$/*Il6ra*$^{fl/fl}$ mice (67.95%) (Fig. 3*C*). No differences were seen between WT and *Il6ra*$^{fl/fl}$ mice lacking Cre (data not shown). It is also noteworthy that macrophages, granulocytes, and hepatocytes together apparently account for almost all of the circulating IL-6Rα in unchallenged mice, because the sum of the proportional

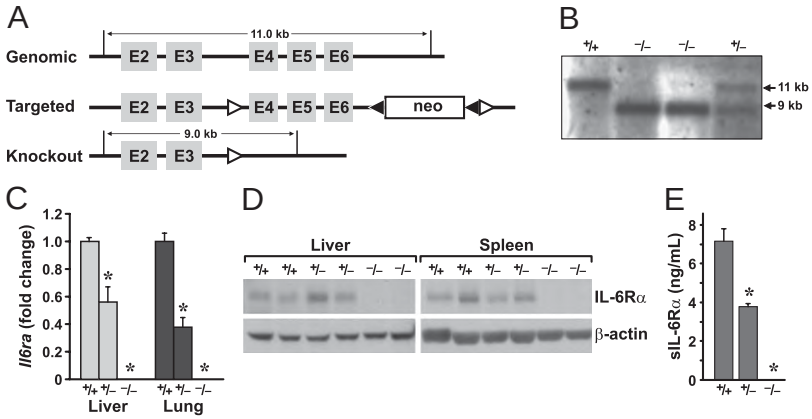

FIGURE 1. Generation of *IL-6ra*–deficient mice. *A*, Schematic depicting exons 2–6 of the genomic *IL-6ra* gene, the targeted construct containing LoxP sites (△) around exons 4–6 and a neo cassette, and the recombined allele after Cre recombinase-mediated excision. *B*, Southern blot analysis of tail DNA from WT, homozygous, and heterozygous *IL-6ra*–targeted alleles, indicating expected band sizes of 11 kb (WT) and 9 kb (knockout). *C*, Real-time PCR with primers specific for exon 5 of murine *IL-6ra* indicating an absence of *IL-6ra* RNA in homozygous knockout mice. Data are expressed as fold change relative to WT mice. *D*, Western blot analysis of liver and spleen tissue collected from mice (two of each genotype) with WT, heterozygous, and homozygous alleles for IL-6Rα. *E*, Absence of sIL-6Rα in plasma of homozygous $Il6ra^{-/-}$ mice ($n = 12$) but not in $Il6ra^{+/+}$ ($n = 11$) or $Il6ra^{+/-}$ mice ($n = 12$), as measured by ELISA. $*p < 0.05$. sIL-6R, soluble IL-6R.

deficits in circulating IL-6Rα in $AlbCre^{+/+}/Il6ra^{fl/fl}$ (30.6% deficit) and $LysMCre^{+/-}/Il6ra^{fl/fl}$ (62.7% deficit) mice equaled 93.4% of the levels in WT mice. To determine the contributions of hepatocytes and immune cells to soluble IL-6Rα during inflammatory challenge, plasma and livers were collected from mice subjected to turpentine injection or cutaneous wounding. Despite increased expression of mRNA for *IL-6ra* in livers of WT mice subjected to acute-phase protein induction (Ref. 45 and our own unpublished data), no increase in the expression of soluble IL-6Rα was seen in mice challenged with turpentine or cutaneous wounding (Fig. 3*C*, 3*D*).

We next compared acute-phase reactants in mice with conditional expression of IL-6Rα. As expected, generation of an acute-phase response was completely muted in $AlbCre^{+/+}/Il6ra^{fl/fl}$ mice compared with WT or $Il6ra^{fl/fl}$ mice (Fig. 3*E*, 3*F*). This is consistent with hepatocytes being the predominant cell type responsible for acute-phase responses. No significant difference was seen between $LysMCre^{+/-}/Il6ra^{fl/fl}$ mice and WT (Fig. 3*E*, 3*F*) or $LysMCre^{-/-}/Il6ra^{fl/fl}$ mice (data not shown). Despite in vitro reports that soluble IL-6Rα can enhance acute-phase protein expression in HepG2 cells (46), no hepatic acute-phase response was detected in $AlbCre^{+/+}/Il6ra^{fl/fl}$ mice despite their having two-thirds of the WT expression of soluble IL-6Rα (Fig. 3*C*, 3*D*). Apparently, membrane-bound IL-6Rα is essential for the hepatic acute-phase response to IL-6.

The deficit in wound healing is not as severe in $Il6ra^{-/-}$ mice as in $Il6^{-/-}$ mice

It has previously been reported that wound healing is markedly delayed in $Il6^{-/-}$ mice (36, 37). We generated full-thickness small and large excision wounds to determine whether IL-6Rα $^{-/-}$ mice shared a similar phenotype. To our surprise, we found that $Il6ra^{-/-}$ mice did not share the same dramatic delay in wound healing seen

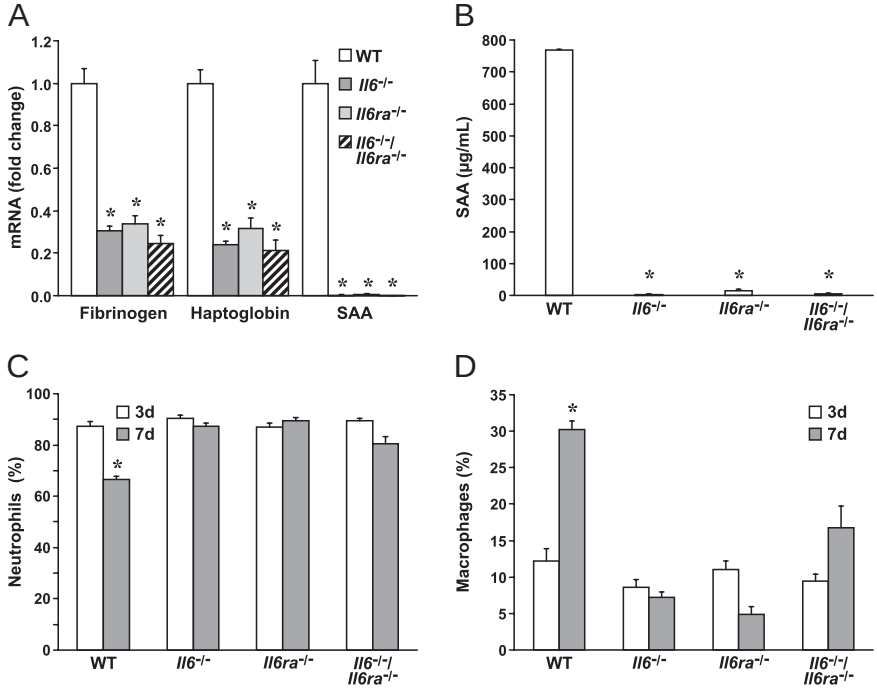

FIGURE 2. $Il6ra^{-/-}$ and $Il6^{-/-}$ mice share a functional deficit in IL-6 signaling. A dramatic reduction in acute-phase protein production in response to turpentine challenge was seen in $Il6ra^{-/-}$ and $Il6^{-/-}$ mice by real-time RT-PCR of liver RNA (*A*) and SAA ELISA of plasma (*B*). *C* and *D*, Differential counts were performed on Kwik-diff–stained cells withdrawn from a sterile inflammatory air pouch lesion induced by carrageenan. Resolution of neutrophils (*C*) and increased influx of monocyte/macrophages (*D*) occurs in WT mice by day 7 but are delayed in $Il6^{-/-}$ and $Il6ra^{-/-}$ mice. Data are expressed as a percentage of total cells.

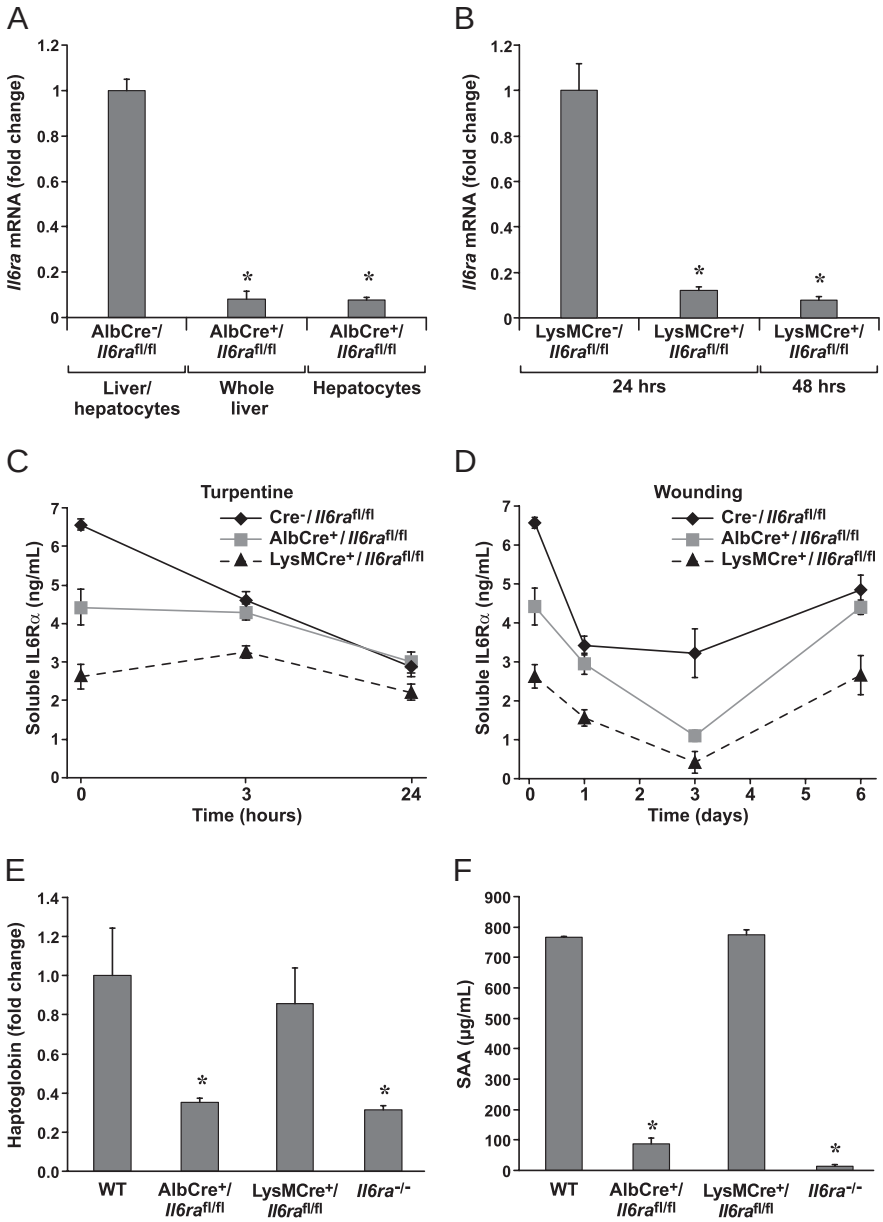

FIGURE 3. Macrophages, neutrophils, and hepatocytes make a significant contribution to circulating levels of soluble IL-6Rα and to acute-phase responses. Knockdown of IL-6Rα was confirmed by RT-PCR in $Il6ra^{fl/fl}$ mice bred with mice expressing Cre recombinase under the control of the albumin promoter (*A*) or the lysozyme M promoter (*B*), as compared with $Il6ra^{fl/fl}$ mice lacking Cre expression. Isolated hepatocytes and whole-liver homogenates were used to test for *IL-6ra* mRNA expression in $AlbCre^{+/+}/Il6ra^{-/-}$ mice. Thioglycolate-elicited peritoneal cells were collected from $LysMCre^{+/-}/Il6ra^{-/-}$ mice after 24 and 48 h and enriched for macrophages by adherence to plastic. *C* and *D*, Expression of soluble IL-6Rα was reduced in plasma of mice with Cre-mediated deletion of *IL-6ra* (time 0) and further diminished, proportionately, after challenge with turpentine (*C*) or by cutaneous wounding (*D*). *E* and *F*, Acute phase reactions following turpentine challenge were diminished in mice lacking *IL-6ra* in hepatocytes but not in granulocytes, as assessed by mRNA for hepatic haptoglobin (*E*) and plasma SAA protein (*F*). $*p < 0.05$; $**p < 0.0001$.

in $Il6^{-/-}$ mice. Instead, $Il6ra^{-/-}$ mice with large excision wounds healed almost as well as WT mice upon gross examination (Fig. 4*A*). $Il6^{-/-}$ mice exhibited reduced wound closure rates and frequently had open wounds for several days longer than WT or $Il6ra^{-/-}$ mice (Fig. 5*A*). Differences in small biopsy punch wounds (4 mm in diameter) were subtle, as wounds healed rapidly (data not shown). However, large wounds of $Il6^{-/-}$ mice frequently became expanded beyond the boundaries of the original wound (Fig. 4*A*), presumably by scratching or dragging of the wound with the mouse's limbs. This assumption was made because the extended edge of the wound was always on the caudal edge, which is more accessible to the legs of mice, and because this action was occasionally observed. Ulcers generated from this activity were seen in only one WT mouse (1 of 12 mice; 8%) with resolution within 24 h. $Il6^{-/-}$ mice all developed ulcers (12 of 12 mice, 100%), which had not healed at 8 d but were healing in some mice by the 11th day. Only 2 of 11 $Il6ra^{-/-}$ mice (18%) developed ulcers adjacent to the wound area, and both were resolved within 24 h. Whether the formation of these ulcers was prompted by prolonged irritation from an open wound, psychological/stress-induced defects in $Il6^{-/-}$ mice (47), or phenotypic defects in wound contraction was not determined.

Histological evaluation of the wound was performed to quantify differences in the multiple processes involved in successful wound healing. Re-epithelialization was markedly delayed in both $Il6^{-/-}$ and $Il6ra^{-/-}$ mice compared with WT mice in both large (Figs. 4*B*, 5*C*) and small wounds (Fig. 5*D*). Separate experiments performed in mice with conditional expression of IL-6Rα indicated that hepatic expression of IL-6Rα was more important for re-epithelialization than that of myeloid cells (Fig. 5*E*). Delayed re-epithelialization in $Il6ra^{-/-}$ mice was an unexpected finding because macroscopic wound closure rates were similar to WT mice. Instead, wound contraction rates were similar in WT and $Il6ra^{-/-}$ mice but delayed in $Il6^{-/-}$ mice, accounting for the macroscopic observation of a smaller defect in $Il6ra^{-/-}$ mice than in $Il6^{-/-}$ mice (Fig. 5*A*, 5*B*). Deficits in the formation of granulation tissue were seen in both $Il6^{-/-}$ and $Il6ra^{-/-}$ mice but were more pronounced in $Il6^{-/-}$ mice. Deficits included delays in macrophage infiltration (Fig. 4*C*, 4*D*), fibrin clearance (Fig. 4*E*), and vascularization (Fig. 4*F*). These deficits have previously been

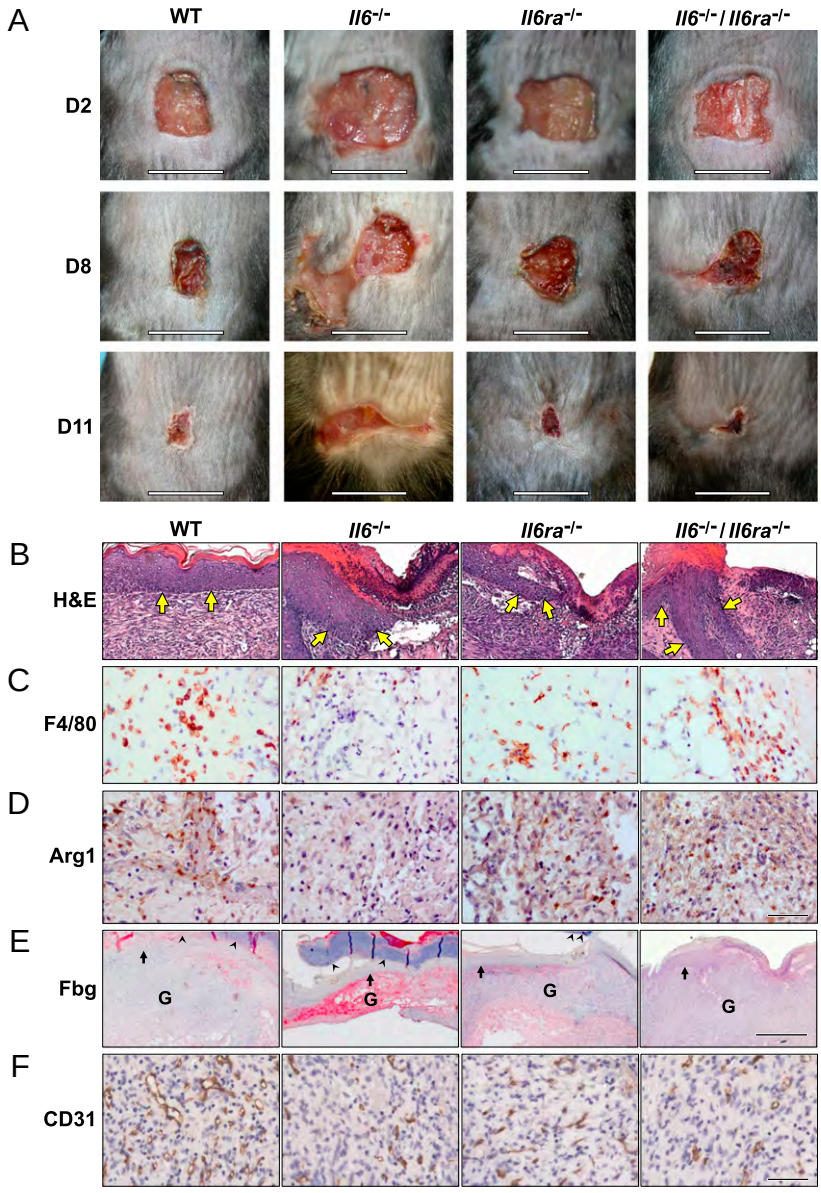

FIGURE 4. Cutaneous wound healing occurs more efficiently in *Il6ra*$^{-/-}$ and *Il6*$^{-/-}$/*Il6ra*$^{-/-}$ mice than in *Il6*$^{-/-}$ mice. *A*, Photomicrographs of large excision wounds made in dorsal skin after 2, 8, and 11 d. Scale bar, 1 cm. *B*, H&E sections indicating complete re-epithelialization (arrows) in WT mice and impaired re-epithelialization in other groups of mice (arrows) 11 d after large excisional wounding (original magnification ×100). *C–F*, Immunohistochemical analysis of large wounds for macrophages [F4/80 Ab, day 6 (*C*); arginase 1 (Arg1), day 5 (*D*); and fibrinogen (fbg, day 8, pink/red reaction product) (*E*)]. "G" indicates granulation tissue, arrows indicate the newly formed epithelial layer, and arrowheads point to the superficial eschar. *F*, Blood vessels were indicated by immunohistochemistry for CD31 (PECAM, day 5). Scale bar, 100 μM (*D, F*); 500 μM (*E*). Original magnification ×400 (*C*, *D*, *F*) and ×25 (*E*). Arg1, arginase 1; fbg, fibrinogen.

reported in *Il6*$^{-/-}$ mice (37, 48). Both fibrin clearance and granulation tissue formation can be attributed to macrophage activity in healing wounds. Granulation tissue formation in *Il6ra*$^{-/-}$ and *Il6*$^{-/-}$/*Il6ra*$^{-/-}$ mice was variable and ranged from being similar to WT to the severe deficits seen in *Il6*$^{-/-}$ mice. However, large wounds of *Il6*$^{-/-}$ mice consistently displayed the most severely impaired wound healing with regard to all parameters studied except re-epithelialization (Figs. 4, 5*A*, 5*B*).

As differences were seen in wound healing between *Il6*$^{-/-}$ and *Il6ra*$^{-/-}$ mice, we wanted to determine whether IL-6 uses another receptor in the absence of IL-6Rα or whether the absence of the receptor itself may account for the improved wound-healing phenotype in *Il6ra*$^{-/-}$ mice. Some promiscuity exists in the IL-6 family of cytokines as high concentrations of CNTF or the IL-27 subunit p28 have been shown to induce a low level of signaling through IL-6Rα (1, 2, 49), and differing phenotypes have been reported between receptor and ligand knockouts for CNTF. However, mammalian IL-6 is not known to have any activity independent of IL-6Rα. We hypothesized that if IL-6 could signal through another receptor, then wound healing would be expected to be delayed in mice with a combined deficit of IL-6 and IL-6Rα. Instead, closure of large excisional wounds in *Il6*$^{-/-}$/*Il6ra*$^{-/-}$ mice occurred on a time frame most similar to *Il6ra*$^{-/-}$ mice, as did the formation of granulation tissue (Fig. 4). Apparently, absence of the receptor is more important for rescuing wound healing in *Il6ra*$^{-/-}$ mice than is promiscuous IL-6 activity.

To confirm that the depletion of IL-6Rα improves wound contraction in *Il6*$^{-/-}$ mice, we treated mice with Abs specific for IL-6Rα and gp130. As expected, depletion of gp130 delayed wound contraction in WT mice (Fig. 5*F*, 5*G*), consistent with its previously defined role in wound healing (50) but had no effect on *Il6*$^{-/-}$ mice (data not shown). However, although depletion of circulating IL-6Rα did not affect wound contraction in WT mice, it dramatically improved wound contraction in *Il6*$^{-/-}$ mice (Fig. 5*F*, 5*G*), similar to data obtained in mice with a combined genetic deficit of IL-6 and IL-6Rα. These data are consistent with the notion that IL-6Rα both facilitates wound healing in an IL-6–dependent fashion but also impairs wound healing in a manner that does not involve IL-6. To determine whether IL-27 p28 binding to IL-6Rα accounts for this negative effect of IL-6Rα in wound contraction, we treated mice with an Ab specific for murine p28. The dose used was sufficient to prevent exogenous p28 from inducing primary murine macrophages from expressing IL-10 and suppressing IL-17 in vitro (data not shown). No difference in

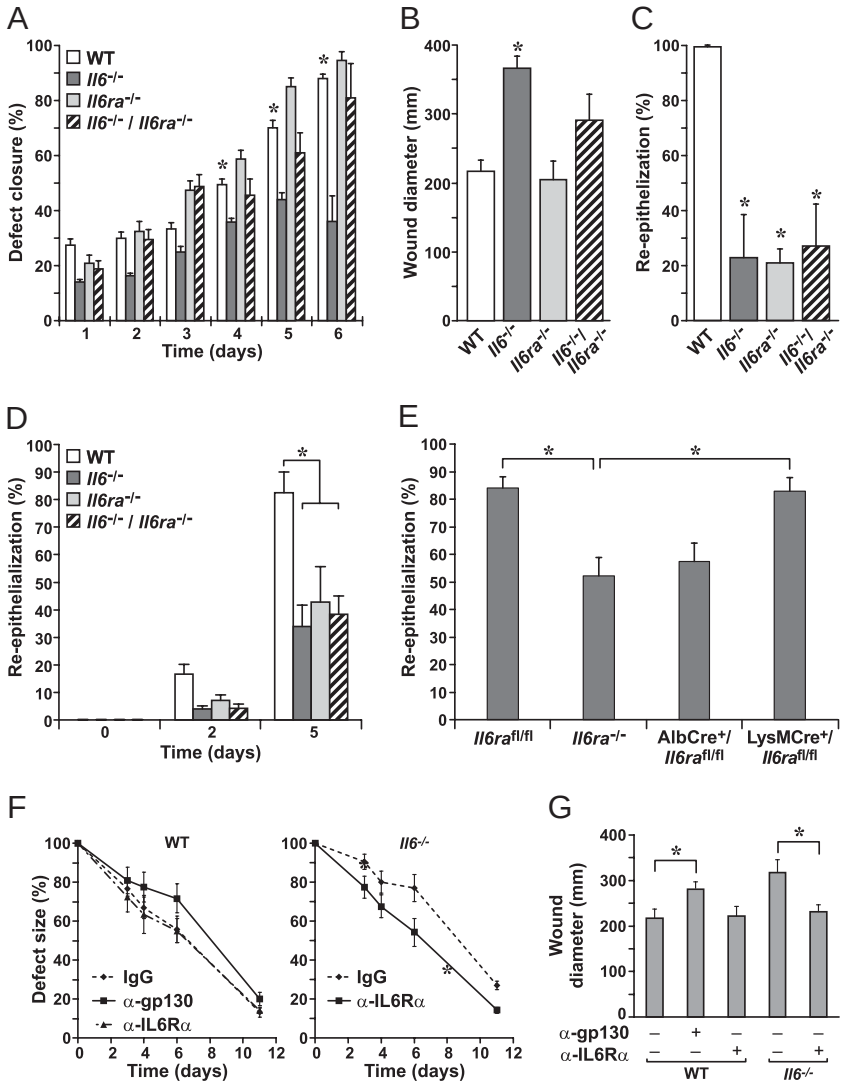

FIGURE 5. Cutaneous wounds in *Il6ra*$^{-/-}$ mice contract similarly to WT mice but display delayed re-epithelialization. Wound-closure rates in mice were quantified superficially (*A*) by placing a 1-cm^2 grid over large excisional wounds and microscopically (*B*) by measuring the width of the granulation tissue in histological preparations taken from the center of large wounds. *C* and *D*, Re-epithelialization was assessed in H&E preparations as the percentage of the wound surface over the newly formed granulation tissue that is covered by keratinocytes in large wounds at day 11 (*C*) and in small punch biopsy wounds after 0, 2, and 5 d (*D*). *E*, Re-epithelialization is delayed to a greater extent in AlbCre$^{+/+}$/*Il6ra*$^{-/-}$ mice than in LysMCre$^{+/-}$/*Il6ra*$^{-/-}$ mice. Small punch wound after 5 d. *F*, Large wounds were generated in WT (*left panel*) and *Il6*$^{-/-}$ mice (*right panel*) prior to daily i.p. administration of control Ab (IgG) or Abs specific for mouse gp130 or mouse IL-6Rα, and wound contraction was assessed macroscopically. *G*, Wound diameter was assessed macroscopically 11 d after wounding and daily treatment with Abs, as shown.

wound contraction was seen with this treatment in either WT or *Il6*$^{-/-}$ mice (data not shown).

To identify a mechanism that could explain the timely wound healing observed in the absence of IL-6Rα regardless of the presence or absence of IL-6, we investigated signaling pathways known to be induced by IL-6Rα signaling. Stat3 phosphorylation was reduced to a similar extent in *Il6*$^{-/-}$, *Il6ra*$^{-/-}$, and *Il6*$^{-/-}$/*Il6ra*$^{-/-}$ mice (Fig. 6*A*) compared with WT mice at 30 min after wounding and is therefore unlikely to explain differences between genotypes. At later time points, Stat3 phosphorylation in knockout mice was not different from that in WT mice (data not shown). However, phosphorylation of the MAPK ERK1/2 was undetectable in *Il6*$^{-/-}$ mice yet increased in *Il6ra*$^{-/-}$ relative to WT mice 1 d after wounding (Fig. 6*A*). ERK phosphorylation in *Il6*$^{-/-}$/*Il6ra*$^{-/-}$ was similar to that of WT mice but notably higher than that of *Il6*$^{-/-}$ mice. Given the importance of ERK activation in promoting wound healing, we wondered whether ERK activation could account for the difference seen between mice lacking IL-6 or IL-6Rα. To test this hypothesis, we treated mice with a MEK1/2 inhibitor (U0126) to prevent ERK activation. Topical application of U0126 reduced ERK phosphorylation in wounds of both WT and *Il6ra*$^{-/-}$ mice compared with vehicle-treated controls (Fig. 6*B*). The difference in wound contraction rates was significantly delayed in *Il6ra*$^{-/-}$ mice treated with U0126 compared with vehicle control-treated mice but did not reach significance in WT mice (Fig. 6*C*). These data suggest that, despite diminished Stat3 activation in *Il6*$^{-/-}$ and *Il6ra*$^{-/-}$ mice, enhanced ERK activation in *Il6ra*$^{-/-}$ mice may rescue wound contraction.

Discussion

In this paper, we provide the first report of mice with a complete deficiency of IL-6Rα and of mice with conditional deletion of IL-6Rα. *Il6ra*$^{-/-}$ mice share many of the phenotypic abnormalities reported in *Il6*$^{-/-}$ mice. However, *Il6ra*$^{-/-}$ mice do not display the dramatic delay in wound healing seen in *Il6*$^{-/-}$ mice. Wound healing in mice with a combined deficit of IL-6 and IL-6Rα resembles wound healing in WT and *Il6ra*$^{-/-}$ mice more than that in *Il6*$^{-/-}$ mice, suggestive of a previously unknown role for IL-6Rα that does not involve IL-6.

Similar to *Il6*$^{-/-}$ mice, *Il6ra*$^{-/-}$ mice show deficiencies in the modulation of inflammatory responses. Using a model of sterile inflammation, we show that *Il6ra*$^{-/-}$ mice demonstrate a similar defect in neutrophil resolution and in progression to a macrophage-dominated response as *Il6*$^{-/-}$ mice. Similarly, mice of both genotypes share a complete inability to generate an acute-phase response after inflammatory challenge with turpentine. Mice with a conditional deletion of IL-6Rα in hepatocytes but not in macrophages or granulocytes shared the inability of *Il6ra*$^{-/-}$ mice to generate a response to turpentine. These results confirm the importance of the hepatocyte in this response and indicate that

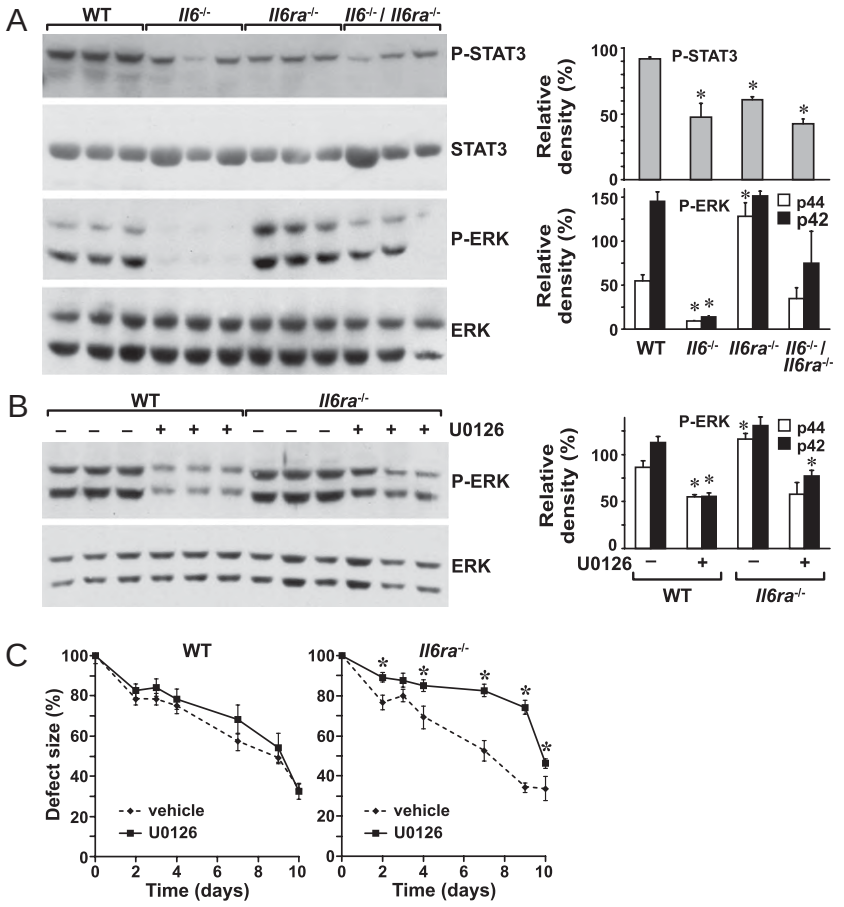

FIGURE 6. ERK activation is increased in *Il6ra*$^{-/-}$ mice compared with WT mice. *A*, Total and phosphorylated (p) Stat3 and ERK were assessed in small punch biopsy wounds collected after 30 min (Stat3) or 1 d (ERK) by Western blotting. Densitometry results for the blots are provided to the *right*. $*p < 0.05$. *B*, Total and p-ERKs were assessed in small wounds generated in WT and *Il6ra*$^{-/-}$ mice treated topically with vehicle (DMSO) or with the MEK inhibitor U0126. Wounds were harvested after 1 d, and western blotting was performed on lysates. *C*, Wound contraction was assessed macroscopically in large wounds of WT (*left panel*) and *Il6ra*$^{-/-}$ mice treated daily with vehicle (DMSO) or U0126. $*p < 0.05$.

soluble IL-6Rα expression by inflammatory cells is neither required nor sufficient. Given that mice with IL-6Rα deficiency in hepatocytes still have almost two-thirds of the levels of circulating soluble IL-6Rα as WT mice yet have the same defect in generating an acute-phase response as *Il6ra*$^{-/-}$ mice, we conclude that membrane-bound IL-6Rα on hepatocytes is essential for the acute-phase response.

Through studies in mice with conditional expression of IL-6Rα, we demonstrated that macrophages and granulocytes produce the majority of soluble circulating IL-6Rα (62.7%) in unchallenged and challenged mice and that hepatocytes produce most of the remainder (30.6%). The greater contribution by immune cells is consistent with immune cell-derived IL-6Rα being secreted and transported to distant inflammatory sites. Soluble IL-6Rα delivered to an inflammatory area allows IL-6 signaling through all cells present and, hence, a rapid response to injury or infection. Hepatic expression of IL-6Rα, however, appears to be more relevant to cell-type–specific rapid acute-phase responses specifically mediated by hepatocytes. However, it should be noted that differences in soluble IL-6Rα expression may exist in mice and humans, because mice are restricted to proteolytic cleavage and do not produce the differentially spliced form. It is of interest that the combined hepatic and granulocytic contribution of IL-6Rα apparently accounts for almost all (93.4%) of the soluble IL-6Rα expression in mice. It is possible that compensation from other compartments may occur in mice lacking IL-6Rα in particular cell types or that incomplete knockdown of IL-6Rα in macrophages and granulocytes with the lysozyme M promoter [95–99% efficiency in mature cells; 75–79% efficiency in bone marrow-derived cells (40)] accounts for residual IL-6Rα expression. However, the finding that macrophages, granulocytes, and hepatocytes are the major producers of soluble IL-6Rα is consistent with tissue expression studies (51). Our study did not address lymphocyte production of soluble IL-6Rα, but it is likely that these cells produce the remaining circulating IL-6Rα in unchallenged mice and that their production increases during immune responses (52).

On the basis of the similarities that we found between the phenotypes of *Il6*$^{-/-}$ and *Il6ra*$^{-/-}$ mice, it was somewhat surprising to find differences between these genotypes in wound-healing responses. Inflammation is an influential part of wound healing, and early granulation tissue contains many of the inflammatory cell types, cytokines, and angiogenic vessels typical of inflammation. Deficits in macrophage infiltration and subsequent fibrin clearance in *Il6*$^{-/-}$ mice were not typical in wounds of *Il6ra*$^{-/-}$ mice. The improved wound-healing phenotype in IL-6Rα$^{-/-}$ mice indicates a divergence in functionality between IL-6 and IL-6Rα and possibly a compensatory mechanism in the absence of IL-6Rα. As mice with a combined deficiency of IL-6 and IL-6Rα demonstrated a wound-healing phenotype closely aligned with that of *Il6ra*$^{-/-}$ mice, it is likely that the absence of IL-6Rα played a greater role in rescuing the phenotype in *Il6ra*$^{-/-}$ mice than did IL-6 promiscuity. However, mice with both deficits did not heal as efficiently as *Il6ra*$^{-/-}$ mice. Therefore, we cannot eliminate the possibility that IL-6 may also signal through a different receptor in these mice.

Many interrelated processes involved in wound healing were improved in *Il6ra*$^{-/-}$ mice compared with *Il6*$^{-/-}$ mice, including macrophage infiltration, fibrin clearance, and angiogenesis. That re-epithelialization was delayed in both *Il6*$^{-/-}$ and *Il6ra*$^{-/-}$ mice was surprising given the differences in wound closure rates. It seems that restored wound contraction and granulation tissue formation in *Il6ra*$^{-/-}$ mice accounts for the appearance that wounds are healing

efficiently, despite the delay in keratinocyte migration over the wound bed. Interestingly, experiments in mice with conditional expression of IL-6Rα indicated that hepatocyte IL-6Rα was more important in cutaneous wound re-epithelialization than that of macrophages and granulocytes. This finding is unexpected given that most circulating IL-6Rα comes from macrophages and granulocytes and because these cell types are numerous in healing wounds. Apparently, one or more of the numerous acute-phase reactants or growth factors produced by the liver in response to IL-6 contribute to re-epithelialization.

In both knockout mice and Ab-depletion studies, we showed that depletion of IL-6Rα rescues wound healing in *Il6*$^{-/-}$ mice. No difference in Stat3 phosphorylation was seen between any of the wounds in the knockout mice, which in each case was less than the phosphorylated Stat3 observed in WT mice. Similarly, the lack of re-epithelialization in both *Il6*$^{-/-}$ and *Il6ra*$^{-/-}$ mice, a Stat3-dependent process, argues against this mechanism alone accounting for the rescued wound healing observed in *Il6ra*$^{-/-}$ mice. Our data imply that IL-6Rα contributes positively to wound healing in an IL-6– and Stat3-dependent manner but potentially hinders wound contraction in an IL-6–independent fashion. This mechanism is unlikely to involve other IL-6 family ligands because they predominantly induce Jak/Stat signaling. However, because select ligands in the IL-6 family, specifically IL-27 p28 and CNTF, have been shown to mediate low-affinity binding to IL-6Rα in vitro (1, 2), we investigated the effect of blocking IL-27 p28 in vivo. We reasoned that if the interaction of this ligand with IL-6Rα accounted for the inhibitory effects of wound contraction by IL-6Rα, then blocking p28 with a specific Ab should rescue wound contraction in *Il6*$^{-/-}$ mice. Instead, no differences in wound contraction were seen in either WT or *Il6*$^{-/-}$ mice treated with Abs to p28. CNTF blocking experiments were not performed because CNTF production is restricted to glial and CNS cells, and CNTF does not possess a signal peptide for secretion. Instead, we investigated ERK activation as both a downstream mediator of IL-6Rα signaling (13, 53, 54) and as an important effector of wound contraction (55). ERK phosphorylation was increased in wounds of *Il6ra*$^{-/-}$ mice but not *Il6*$^{-/-}$ mice, and blocking ERK activation with a MEK inhibitor delayed wound healing in *Il6ra*$^{-/-}$ mice. These data suggest that increased ERK activation increases wound contraction in *Il6ra*$^{-/-}$ mice but not in *Il6*$^{-/-}$ mice. We observed that topical application of the MEK inhibitor U0126 inhibited wound contraction to a greater extent in *Il6ra*$^{-/-}$ mice than in WT mice. Although it is tempting to speculate that wound healing in the absence of IL-6Rα may be more dependent on ERK activation than in WT mice, such a conclusion would be premature, because more studies are needed to determine the contributions of the MAPK or other signaling pathways and mechanisms to the healing process in *Il6ra*$^{-/-}$ mice. In addition, it should be noted that the importance of such a mechanism remains to be determined, because it may prove to be specific to mice or may occur only in the context of the nonphysiological absence of IL-6Rα.

Questions still remain regarding the mechanism by which deletion of IL-6Rα could lead to increased ERK activation, independently of IL-6 signaling. It could be that IL-6Rα plays a role in gp130 internalization and membrane expression, or a cytoplasmic phosphorylation site of IL-6Rα (56) may be involved in ERK suppression in the wound microenvironment. Sparse data suggest that gp130 and/or IL-6Rα interact with several adaptor proteins upstream of ERK activation, such as Grb1, Src homology region 2 domain-containing phosphatase 2, Vav, and Src family kinases (8, 53, 57–60). The depletion of IL-6Rα protein may deregulate the balance between these positive and negative effectors of the MAPK pathway, leading to increased ERK activation. In support of this idea, treatment of HepG2 cells with soluble IL-6Rα in the absence of IL-6 led to a complete inhibition of early growth response protein 1, a gene downstream of ERK activation (61). Similarly, cross-talk between gp130 and/or IL-6Rα and the EGF family receptors has been reported in several tumor cell lines (62–66) and in primary mammary epithelial cells (67). It is also possible that increased ERK activation in the absence of IL-6Rα is due to indirect effects on the expression or activity of other cytokines or on receptors other than gp130. It is not clear what the effect of IL-6Rα deficiency would have on these interactions. However, given the similarity between healing wounds and the tumor microenvironment and given that Abs against IL-6Rα are already in clinical usage in patients with rheumatic diseases, there is a strong rationale for better understanding this novel role for IL-6Rα in regulating ERK activation.

Acknowledgments

We thank the University of Cincinnati Gene-Targeted Mouse Service for expert assistance with generating the *Il6ra*-targeted mice, Dr. Mark Magnusen for the EIIa-Cre mice, Dr. Jay L. Degen for the rabbit anti-mouse fibrinogen Ab, and Drs. Simon A. Jones and Patrick B. Dennis for advice. Expert graphical and editorial assistance was provided by Glenn Doerman and Maryellen Daston, respectively.

Disclosures

The authors have no financial conflicts of interest.

References

1. Schuster, B., M. Kovaleva, Y. Sun, P. Regenhard, V. Matthews, J. Grötzinger, S. Rose-John, and K. J. Kallen. 2003. Signaling of human ciliary neurotrophic factor (CNTF) revisited: the interleukin-6 receptor can serve as an α-receptor for CTNF. *J. Biol. Chem.* 278: 9528–9535.
2. Crabé, S., A. Guay-Giroux, A. J. Tormo, D. Duluc, R. Lissilaa, F. Guilhot, U. Mavoungou-Bigouagou, F. Lefouili, I. Cognet, W. Ferlin, et al. 2009. The IL-27 p28 subunit binds cytokine-like factor 1 to form a cytokine regulating NK and T cell activities requiring IL-6R for signaling. *J. Immunol.* 183: 7692–7702.
3. Taga, T., M. Hibi, Y. Hirata, K. Yamasaki, K. Yasukawa, T. Matsuda, T. Hirano, and T. Kishimoto. 1989. Interleukin-6 triggers the association of its receptor with a possible signal transducer, gp130. *Cell* 58: 573–581.
4. Bravo, J., and J. K. Heath. 2000. Receptor recognition by gp130 cytokines. *EMBO J.* 19: 2399–2411.
5. Murakami, M., M. Hibi, N. Nakagawa, T. Nakagawa, K. Yasukawa, K. Yamanishi, T. Taga, and T. Kishimoto. 1993. IL-6–induced homodimerization of gp130 and associated activation of a tyrosine kinase. *Science* 260: 1808–1810.
6. Lütticken, C., U. M. Wegenka, J. Yuan, J. Buschmann, C. Schindler, A. Ziemiecki, A. G. Harpur, A. F. Wilks, K. Yasukawa, T. Taga, et al. 1994. Association of transcription factor APRF and protein kinase Jak1 with the interleukin-6 signal transducer gp130. *Science* 263: 89–92.
7. Stahl, N., T. G. Boulton, T. Farruggella, N. Y. Ip, S. Davis, B. A. Witthuhn, F. W. Quelle, O. Silvennoinen, G. Barbieri, S. Pellegrini, et al. 1994. Association and activation of Jak-Tyk kinases by CNTF-LIF-OSM-IL-6β receptor components. *Science* 263: 92–95.
8. Stahl, N., T. J. Farruggella, T. G. Boulton, Z. Zhong, J. E. Darnell, Jr., and G. D. Yancopoulos. 1995. Choice of STATs and other substrates specified by modular tyrosine-based motifs in cytokine receptors. *Science* 267: 1349–1353.
9. Haan, S., J. F. Keller, I. Behrmann, P. C. Heinrich, and C. Haan. 2005. Multiple reasons for an inefficient STAT1 response upon IL-6–type cytokine stimulation. *Cell. Signal.* 17: 1542–1550.
10. Wegenka, U. M., J. Buschmann, C. Lütticken, P. C. Heinrich, and F. Horn. 1993. Acute-phase response factor, a nuclear factor binding to acute-phase response elements, is rapidly activated by interleukin-6 at the posttranslational level. *Mol. Cell. Biol.* 13: 276–288.
11. Fukada, T., M. Hibi, Y. Yamanaka, M. Takahashi-Tezuka, Y. Fujitani, T. Yamaguchi, K. Nakajima, and T. Hirano. 1996. Two signals are necessary for cell proliferation induced by a cytokine receptor gp130: involvement of STAT3 in anti-apoptosis. *Immunity* 5: 449–460.
12. Ohtani, T., K. Ishihara, T. Atsumi, K. Nishida, Y. Kaneko, T. Miyata, S. Itoh, M. Narimatsu, H. Maeda, T. Fukada, et al. 2000. Dissection of signaling cascades through gp130 in vivo: reciprocal roles for STAT3- and SHP2-mediated signals in immune responses. *Immunity* 12: 95–105.
13. Ernst, M., and B. J. Jenkins. 2004. Acquiring signalling specificity from the cytokine receptor gp130. *Trends Genet.* 20: 23–32.

14. Rose-John, S., J. Scheller, G. Elson, and S. A. Jones. 2006. Interleukin-6 biology is coordinated by membrane-bound and soluble receptors: role in inflammation and cancer. *J. Leukoc. Biol.* 80: 227–236.
15. Müllberg, J., H. Schooltink, T. Stoyan, P. C. Heinrich, and S. Rose-John. 1992. Protein kinase C activity is rate limiting for shedding of the interleukin-6 receptor. *Biochem. Biophys. Res. Commun.* 189: 794–800.
16. Horiuchi, S., Y. Koyanagi, Y. Zhou, H. Miyamoto, Y. Tanaka, M. Waki, A. Matsumoto, M. Yamamoto, and N. Yamamoto. 1994. Soluble interleukin-6 receptors released from T cell or granulocyte/macrophage cell lines and human peripheral blood mononuclear cells are generated through an alternative splicing mechanism. *Eur. J. Immunol.* 24: 1945–1948.
17. Jones, S. A., S. Horiuchi, D. Novick, N. Yamamoto, and G. M. Fuller. 1998. Shedding of the soluble IL-6 receptor is triggered by Ca^{2+} mobilization, while basal release is predominantly the product of differential mRNA splicing in THP-1 cells. *Eur. J. Immunol.* 28: 3514–3522.
18. Peters, M., S. Jacobs, M. Ehlers, P. Vollmer, J. Müllberg, E. Wolf, G. Brem, K. H. Meyer zum Büschenfelde, and S. Rose-John. 1996. The function of the soluble interleukin 6 (IL-6) receptor in vivo: sensitization of human soluble IL-6 receptor transgenic mice towards IL-6 and prolongation of the plasma half-life of IL-6. *J. Exp. Med.* 183: 1399–1406.
19. Rabe, B., A. Chalaris, U. May, G. H. Waetzig, D. Seegert, A. S. Williams, S. A. Jones, S. Rose-John, and J. Scheller. 2008. Transgenic blockade of Interleukin-6-trans-signaling abrogates inflammation. *Blood* 111: 1021–1028.
20. Chalaris, A., B. Rabe, K. Paliga, H. Lange, T. Laskay, C. A. Fielding, S. A. Jones, S. Rose-John, and J. Scheller. 2007. Apoptosis is a natural stimulus of IL6R shedding and contributes to the proinflammatory trans-signaling function of neutrophils. *Blood* 110: 1748–1755.
21. Hurst, S. M., T. S. Wilkinson, R. M. McLoughlin, S. Jones, S. Horiuchi, N. Yamamoto, S. Rose-John, G. M. Fuller, N. Topley, and S. A. Jones. 2001. IL-6 and its soluble receptor orchestrate a temporal switch in the pattern of leukocyte recruitment seen during acute inflammation. *Immunity* 14: 705–714.
22. McLoughlin, R. M., J. Witowski, R. L. Robson, T. S. Wilkinson, S. M. Hurst, A. S. Williams, J. D. Williams, S. Rose-John, S. A. Jones, and N. Topley. 2003. Interplay between IFN-γ and IL-6 signaling governs neutrophil trafficking and apoptosis during acute inflammation. *J. Clin. Invest.* 112: 598–607.
23. Vermes, C., J. J. Jacobs, J. Zhang, G. Firneisz, K. A. Roebuck, and T. T. Glant. 2002. Shedding of the interleukin-6 (IL-6) receptor (gp80) determines the ability of IL-6 to induce gp130 phosphorylation in human osteoblasts. *J. Biol. Chem.* 277: 16879–16887.
24. Kopf, M., H. Baumann, G. Freer, M. Freudenberg, M. Lamers, T. Kishimoto, R. Zinkernagel, H. Bluethmann, and G. Köhler. 1994. Impaired immune and acute-phase responses in interleukin-6–deficient mice. *Nature* 368: 339–342.
25. Poli, V., R. Balena, E. Fattori, A. Markatos, M. Yamamoto, H. Tanaka, G. Ciliberto, G. A. Rodan, and F. Costantini. 1994. Interleukin-6 deficient mice are protected from bone loss caused by estrogen depletion. *EMBO J.* 13: 1189–1196.
26. Cressman, D. E., L. E. Greenbaum, R. A. DeAngelis, G. Ciliberto, E. E. Furth, V. Poli, and R. Taub. 1996. Liver failure and defective hepatocyte regeneration in interleukin-6–deficient mice. *Science* 274: 1379–1383.
27. Wallenius, V., K. Wallenius, B. Ahrén, M. Rudling, H. Carlsten, S. L. Dickson, C. Ohlsson, and J. O. Jansson. 2002. Interleukin-6–deficient mice develop mature-onset obesity. *Nat. Med.* 8: 75–79.
28. Mendel, I., A. Katz, N. Kozak, A. Ben-Nun, and M. Revel. 1998. Interleukin-6 functions in autoimmune encephalomyelitis: a study in gene-targeted mice. *Eur. J. Immunol.* 28: 1727–1737.
29. Hatzi, E., C. Murphy, A. Zoephel, H. Rasmussen, L. Morbidelli, H. Ahorn, K. Kunisada, U. Tontsch, M. Klenk, K. Yamauchi-Takihara, et al. 2002. N-myc oncogene overexpression down-regulates IL-6; evidence that IL-6 inhibits angiogenesis and suppresses neuroblastoma tumor growth. *Oncogene* 21: 3552–3561.
30. Mulé, J. J., J. K. McIntosh, D. M. Jablons, and S. A. Rosenberg. 1990. Antitumor activity of recombinant interleukin 6 in mice. *J. Exp. Med.* 171: 629–636.
31. Hong, D. S., L. S. Angelo, and R. Kurzrock. 2007. Interleukin-6 and its receptor in cancer: implications for translational therapeutics. *Cancer* 110: 1911–1928.
32. Martin, P., and S. J. Leibovich. 2005. Inflammatory cells during wound repair: the good, the bad and the ugly. *Trends Cell Biol.* 15: 599–607.
33. Simpson, D. M., and R. Ross. 1972. The neutrophilic leukocyte in wound repair a study with antineutrophil serum. *J. Clin. Invest.* 51: 2009–2023.
34. Dovi, J. V., L. K. He, and L. A. DiPietro. 2003. Accelerated wound closure in neutrophil-depleted mice. *J. Leukoc. Biol.* 73: 448–455.
35. Leibovich, S. J., and R. Ross. 1975. The role of the macrophage in wound repair: a study with hydrocortisone and antimacrophage serum. *Am. J. Pathol.* 78: 71–100.
36. Gallucci, R. M., P. P. Simeonova, J. M. Matheson, C. Kommineni, J. L. Guriel, T. Sugawara, and M. I. Luster. 2000. Impaired cutaneous wound healing in interleukin-6–deficient and immunosuppressed mice. *FASEB J.* 14: 2525–2531.
37. Lin, Z. Q., T. Kondo, Y. Ishida, T. Takayasu, and N. Mukaida. 2003. Essential involvement of IL-6 in the skin wound-healing process as evidenced by delayed wound healing in IL-6-deficient mice. *J. Leukoc. Biol.* 73: 713–721.
38. Buchholz, F., P. O. Angrand, and A. F. Stewart. 1998. Improved properties of FLP recombinase evolved by cycling mutagenesis. *Nat. Biotechnol.* 16: 657–662.
39. Postic, C., M. Shiota, K. D. Niswender, T. L. Jetton, Y. Chen, J. M. Moates, K. D. Shelton, J. Lindner, A. D. Cherrington, and M. A. Magnuson. 1999. Dual roles for glucokinase in glucose homeostasis as determined by liver and pancreatic β cell-specific gene knock-outs using Cre recombinase. *J. Biol. Chem.* 274: 305–315.
40. Clausen, B. E., C. Burkhardt, W. Reith, R. Renkawitz, and I. Förster. 1999. Conditional gene targeting in macrophages and granulocytes using LysMcre mice. *Transgenic Res.* 8: 265–277.
41. Berry, M. N., H. J. Halls, and M. B. Grivell. 1992. Techniques for pharmacological and toxicological studies with isolated hepatocyte suspensions. *Life Sci.* 51: 1–16.
42. Drew, A. F., A. H. Kaufman, K. W. Kombrinck, M. J. Danton, C. C. Daugherty, J. L. Degen, and T. H. Bugge. 1998. Ligneous conjunctivitis in plasminogen-deficient mice. *Blood* 91: 1616–1624.
43. Fattori, E., M. Cappelletti, P. Costa, C. Sellitto, L. Cantoni, M. Carelli, R. Faggioni, G. Fantuzzi, P. Ghezzi, and V. Poli. 1994. Defective inflammatory response in interleukin 6-deficient mice. *J. Exp. Med.* 180: 1243–1250.
44. Kaibara, A., N. J. Espat, T. Auffenberg, A. S. Abouhamze, D. Martin, S. Kalra, and L. L. Moldawer. 1998. Interleukin 6, but not ciliary neurotrophic factor or leukaemia inhibitory factor, is responsible for the acute phase response to turpentine-induced myositis. *Cytokine* 10: 452–456.
45. Geisterfer, M., C. Richards, M. Baumann, G. Fey, D. Gywnne, and J. Gauldie. 1993. Regulation of IL-6 and the hepatic IL-6 receptor in acute inflammation in vivo. *Cytokine* 5: 1–7.
46. Mackiewicz, A., H. Schooltink, P. C. Heinrich, and S. Rose-John. 1992. Complex of soluble human IL-6-receptor/IL-6 up-regulates expression of acute-phase proteins. *J. Immunol.* 149: 2021–2027.
47. Butterweck, V., S. Prinz, and M. Schwaninger. 2003. The role of interleukin-6 in stress-induced hyperthermia and emotional behaviour in mice. *Behav. Brain Res.* 144: 49–56.
48. Luckett, L. R., and R. M. Gallucci. 2007. Interleukin-6 (IL-6) modulates migration and matrix metalloproteinase function in dermal fibroblasts from IL-6KO mice. *Br. J. Dermatol.* 156: 1163–1171.
49. Nesbitt, J. E., N. L. Fuentes, and G. M. Fuller. 1993. Ciliary neurotrophic factor regulates fibrinogen gene expression in hepatocytes by binding to the interleukin-6 receptor. *Biochem. Biophys. Res. Commun.* 190: 544–550.
50. Zhu, B. M., Y. Ishida, G. W. Robinson, M. Pacher-Zavisin, A. Yoshimura, P. M. Murphy, and L. Hennighausen. 2008. SOCS3 negatively regulates the gp130-STAT3 pathway in mouse skin wound healing. *J. Invest. Dermatol.* 128: 1821–1829.
51. Jones, S. A., P. J. Richards, J. Scheller, and S. Rose-John. 2005. IL-6 transsignaling: the in vivo consequences. *J. Interferon Cytokine Res.* 25: 241–253.
52. Polgár, A., M. Brózik, S. Tóth, M. Holub, K. Hegyi, A. Kádár, L. Hodinka, and A. Falus. 2000. Soluble interleukin-6 receptor in plasma and in lymphocyte culture supernatants of healthy individuals and patients with systemic lupus erythematosus and rheumatoid arthritis. *Med. Sci. Monit.* 6: 13–18.
53. Schiemann, W. P., J. L. Bartoe, and N. M. Nathanson. 1997. Box 3-independent signaling mechanisms are involved in leukemia inhibitory factor receptor α- and gp130-mediated stimulation of mitogen-activated protein kinase: evidence for participation of multiple signaling pathways which converge at Ras. *J. Biol. Chem.* 272: 16631–16636.
54. Lai, C. F., J. Ripperger, Y. Wang, H. Kim, R. B. Hawley, and H. Baumann. 1999. The STAT3-independent signaling pathway by glycoprotein 130 in hepatic cells. *J. Biol. Chem.* 274: 7793–7802.
55. Hirano, S., R. S. Rees, and R. R. Gilmont. 2002. MAP kinase pathways involving hsp27 regulate fibroblast-mediated wound contraction. *J. Surg. Res.* 102: 77–84.
56. Müllberg, J., W. Oberthür, F. Lottspeich, E. Mehl, E. Dittrich, L. Graeve, P. C. Heinrich, and S. Rose-John. 1994. The soluble human IL-6 receptor: mutational characterization of the proteolytic cleavage site. *J. Immunol.* 152: 4958–4968.
57. Ernst, M., D. P. Gearing, and A. R. Dunn. 1994. Functional and biochemical association of Hck with the LIF/IL-6 receptor signal transducing subunit gp130 in embryonic stem cells. *EMBO J.* 13: 1574–1584.
58. Wang, X. Y., D. K. Fuhrer, M. S. Marshall, and Y. C. Yang. 1995. Interleukin-11 induces complex formation of Grb2, Fyn, and JAK2 in 3T3L1 cells. *J. Biol. Chem.* 270: 27999–28002.
59. Lee, I. S., Y. Liu, M. Narazaki, M. Hibi, T. Kishimoto, and T. Taga. 1997. Vav is associated with signal transducing molecules gp130, Grb2 and Erk2, and is tyrosine phosphorylated in response to interleukin-6. *FEBS Lett.* 401: 133–137.
60. Kim, H., and H. Baumann. 1999. Dual signaling role of the protein tyrosine phosphatase SHP-2 in regulating expression of acute-phase plasma proteins by interleukin-6 cytokine receptors in hepatic cells. *Mol. Cell. Biol.* 19: 5326–5338.
61. Holub, M. C., H. Hegyesi, P. Igaz, A. Polgár, S. Toth, and A. Falus. 2002. Soluble interleukin-6 receptor enhanced by oncostatin M induces major changes in gene expression profile of human hepatoma cells. *Immunol. Lett.* 82: 79–84.
62. Qiu, Y., L. Ravi, and H. J. Kung. 1998. Requirement of ErbB2 for signalling by interleukin-6 in prostate carcinoma cells. *Nature* 393: 83–85.
63. Badache, A., and N. E. Hynes. 2001. Interleukin 6 inhibits proliferation and, in cooperation with an epidermal growth factor receptor autocrine loop, increases migration of T47D breast cancer cells. *Cancer Res.* 61: 383–391.
64. Grant, S. L., A. Hammacher, A. M. Douglas, G. A. Goss, R. K. Mansfield, J. K. Heath, and C. G. Begley. 2002. An unexpected biochemical and functional interaction between gp130 and the EGF receptor family in breast cancer cells. *Oncogene* 21: 460–474.
65. Wang, Y. D., J. De Vos, M. Jourdan, G. Couderc, Z. Y. Lu, J. F. Rossi, and B. Klein. 2002. Cooperation between heparin-binding EGF-like growth factor and interleukin-6 in promoting the growth of human myeloma cells. *Oncogene* 21: 2584–2592.
66. Colomiere, M., A. C. Ward, C. Riley, M. K. Trenerry, D. Cameron-Smith, J. Findlay, L. Ackland, and N. Ahmed. 2009. Cross talk of signals between EGFR and IL-6R through JAK2/STAT3 mediate epithelial-mesenchymal transition in ovarian carcinomas. *Br. J. Cancer* 100: 134–144.
67. Zhao, L., S. Hart, J. Cheng, J. J. Melenhorst, B. Bierie, M. Ernst, C. Stewart, F. Schaper, P. C. Heinrich, A. Ullrich, et al. 2004. Mammary gland remodeling depends on gp130 signaling through Stat3 and MAPK. *J. Biol. Chem.* 279: 44093–44100.